Quantum Crystallography: Current Developments and Future Perspectives

Alessandro Genoni,[a*] Lukas Bučinský,[b] Nicolas Claiser,[c] Julia Contreras-García,[d] Birger Dittrich,[e] Paulina M. Dominiak,[f] Enrique Espinosa,[c] Carlo Gatti,[g1,g2] Paolo Giannozzi,[h] Jean-Michel Gillet,[i] Dylan Jayatilaka,[j] Piero Macchi,[k] Anders Ø. Madsen,[l] Louis J. Massa,[m] Chérif F. Matta,[n1,n2,n3,n4] Kenneth M. Merz Jr.,[o1,o2] Philip N. H. Nakashima,[p] Holger Ott,[q] Ulf Ryde,[r] Karlheinz Schwarz,[s] Marek Sierka,[t] Simon Grabowsky[u*]

[a] Université de Lorraine, CNRS, Laboratoire LPCT, 1 Boulevard Arago, F-57078, Metz, France;

[b] Institute of Physical Chemistry and Chemical Physics, Slovak University of Technology, FCHPT SUT, Radlinského 9, SK-812 37 Bratislava, Slovakia;

[c] Université de Lorraine, CNRS, Laboratoire CRM2, Boulevard des Aiguillettes, BP 70239, F-54506, Vandoeuvre-lès-Nancy, France;

[d] Sorbonne Universités, UPMC Université Paris 06, CNRS, Laboratoire de Chimie Théorique (LCT), 4 Place Jussieu, F-75252 Paris Cedex 05, France;

[e] Anorganische und Strukturchemie II, Heinrich-Heine-Universität Düsseldorf, Universitätsstraße 1, 40225 Düsseldorf, Germany;

[f] Biological and Chemical Research Centre, Department of Chemistry, University of Warsaw, ul. Żwirki i Wigury 101, 02-089, Warszawa, Poland;

[g1] CNR-ISTM Istituto di Scienze e Tecnologie Molecolari, via Golgi 19, Milano, I-20133, Italy;

[g2] Istituto Lombardo Accademia di Scienze e Lettere, via Brera, 28, 20121 Milano, Italy;

[h] Department of Mathematics, Computer Science and Physics, University of Udine, Via delle Scienze 208, I-33100 Udine, Italy;

[i] Structure, Properties and Modeling of Solids Laboratory, CentraleSupelec, Paris-Saclay University, 3 rue Joliot-Curie, 91191 Gif-sur-Yvette, France;

[j] School of Molecular Sciences, University of Western Australia, 35 Stirling Highway, Perth, WA 6009, Australia;

[k] Department of Chemistry and Biochemistry, University of Bern, Freiestrasse 3, CH-3012 Bern, Switzerland;

[l] Department of Pharmacy, University of Copenhagen, Universitetsparken 2, 2100 Copenhagen, Denmark;

[m] Hunter College & the PhD Program of the Graduate Center, City University of New York, New York, USA;

[n1] Department of Chemistry and Physics, Mount Saint Vincent University, Halifax, Nova Scotia B3M 2J6, Canada;

[n2] Department of Chemistry, Dalhousie University, Halifax, Nova Scotia B3H 4J3, Canada;

[n3] Department of Chemistry, Saint Mary's University, Halifax, Nova Scotia B3H 3C3, Canada;

[n4] Département de Chimie, Université Laval, Québec, QC G1V 0A6, Canada;

[o1] Department of Chemistry and Department of Biochemistry and Molecular Biology, Michigan State University, 578 South Shaw Lane, East Lansing, Michigan 48824, USA;

[o2] Institute for Cyber Enabled Research, Michigan State University, 567 Wilson Road, Room 1440, East Lansing, Michigan 48824, USA;

[p] Department of Materials Science and Engineering, Monash University, Victoria 3800, Australia;

[q] Bruker AXS GmbH, Östliche Rheinbrückenstraße 49, 76187 Karlsruhe, Germany;

[r] Department of Theoretical Chemistry, Lund University, Chemical Centre, P. O. Box 124, SE-22100 Lund, Sweden;

[s] Technische Universität Wien, Institut für Materialwissenschaften, Getreidemarkt 9, A-1060 Vienna, Austria;

[t] Otto Schott Institute of Materials Research, Friedrich Schiller University Jena, Löbdergraben 32, 07743 Jena, Germany;

[u] Universität Bremen, Fachbereich 2 – Biologie/Chemie, Institut für Anorganische Chemie und Kristallographie, Leobener Str. 3, 28359 Bremen, Germany.

* Corresponding authors: Alessandro.Genoni@univ-lorraine.fr,
simon.grabowsky@uni-bremen.de

Abstract

Crystallography and quantum mechanics have always been tightly connected because reliable quantum mechanical models are needed to determine crystal structures. Due to this natural synergy, nowadays accurate distributions of electrons in space can be obtained from diffraction and scattering experiments. In the original definition of quantum crystallography (QCr) given by Massa, Karle and Huang, direct extraction of wavefunctions or density matrices from measured intensities of reflections or, conversely, *ad hoc* quantum mechanical calculations to enhance the accuracy of the crystallographic refinement are implicated. Nevertheless, many other active and emerging research areas involving quantum mechanics and scattering experiments are not covered by the original definition although they enable to observe and explain quantum phenomena as accurately and successfully as the original strategies. Therefore, we give an overview over current research that is related to a broader notion of QCr, and discuss options how QCr can evolve to become a complete and independent domain of natural sciences. The goal of this paper is to initiate discussions around QCr, but not to find a final definition of the field.

1. Introduction

Properties of materials as well as modes of action of drugs are directly related to their electronic structure. Therefore, one of the most important challenges in modern science is the accurate determination of the electronic structure, from which structure-function relationships can be derived. One way of obtaining information on electronic structure is by calculating wavefunctions of the materials or compounds under investigation using quantum mechanics. Wavefunctions are mathematical objects that intrinsically contain all the information of quantum mechanical systems in specific pure states. They can be obtained as approximate solutions of the Schrödinger equation (e.g., through numerical calculations) and allow to determine various expectation values that can be directly measured through experiments. Another class of experimental "observables" are available only by means of modeling, namely through optimizations of some parameters that replicate a physical quantity within the assumptions of a given theoretical framework (for example, electron density, magnetization, *etc.*). At the same time, some models based on electron density functions may return partial information also on the wavefunction: for example, an approximate form of the spin part of the wavefunction or an approximate part of the atomic or molecular orbitals. Due to the increasing computational power and the continuing development of sophisticated methods and software, wavefunctions can provide profound insights into electronic distributions and are becoming increasingly important.

Although quantum chemistry has reached great maturity and a broad base of applications, it is worth bearing in mind that even the most rigorous first principle calculations for systems bigger than the hydrogen atom depend on approximations. Therefore, their predictions must find validations. In quantum chemistry, this is particularly cogent because the uncertainty intrinsically associated with the approximation chosen for the calculation is unknown. One can only evaluate the performance of a given theoretical method by using a set of experimental values as benchmarks. In molecular quantum chemistry, the experimental validations often come from spectroscopy. However, in materials science and solid-state chemistry, the best "eye" to probe the quantum behavior of matter is the scattering of

radiation or particles of sufficient energy, typically X-ray, γ-rays, electrons and neutrons. The measured diffraction pattern is a representation of the charge-density distribution in the compound under examination. X-rays and γ-rays interact with the thermally smeared electrons in a crystal, so that one can model either the dynamic electron density or the positive and negative charge-density distributions independently after deconvolution into atomic displacement parameters and static electron density. Neutrons interact with nuclear particles and, therefore, they map the probability distribution of atomic nuclei, from which one can easily derive the positive charge density distribution. Electrons interact with the electrostatic potential generated by electrons and nuclei. There is an additional benefit from measuring scattering of ordered matter, such as crystals (or even quasi-crystals), namely the cooperative effect of molecules, which represents a kind of magnifying lens of the scattering of individual objects.

Thus, theoretical calculations and scattering experiments are complementary approaches to gain insight into the electronic structure of compounds. Actually, X-ray diffraction and wavefunctions have always been intimately related, because modeling crystal structures requires a theoretical framework to interpret the measured data, i.e. charge density is an "observable" available by means of modeling. The simplest model assumes that diffraction is caused by a combination of non-interacting atoms, each of them represented by a spherically averaged ground-state electron density.[1] This model, universally known as *Independent Atom Model* (IAM), implies calculation of atomic wave functions, thus relying on quantum mechanics (QM).[2] The vast majority of modern crystal structure refinements adopts this model to obtain comparably accurate atomic positions and displacement parameters for non-hydrogen atoms.[3,4] However, already in 1915, Debye pointed out that there is more information in the measured X-ray diffraction pattern than the atomic positions. In particular, he recognized that "it should be possible to experimentally determine the special

arrangements of the electrons inside an atom"[1].[5] More than half a century later, this proposal became reality.[6] Today, more accurate crystallographic models are available, which allow to obtain a picture of the "special arrangements of the electrons" (namely, the electron density) from X-ray diffraction measurements.[7]

In this context, besides maximum entropy methods,[8-10] the most popular technique is the atomic multipolar expansion of the electron density, based on the projection of the electron density in atomic terms.[11-15] The multipole model is the result of necessary approximations. In fact, a rigorous treatment of two-center scattering would be quite complicated even for simple compounds, although reported for some diatomic molecules.[16] Furthermore, the modeling of atomic displacements initially led to additional problems in case of two-center electron density functions.[17,18] The one-center expansion led to a much easier formalism, where radial and angular parts derived from atomic orbitals are used as atomic density functions, and where pseudo-atoms are naturally defined.[19] The radial decay of the pseudo-atoms and the core and valence scattering factors in multipole models are directly calculated from wavefunctions and hence the analytical shape of the refined electron density is significantly influenced by quantum chemistry. It is important to mention that, to a good approximation, the set of multipolar orbitals may be related to atomic hybridization states[20] and even to some individual orbital occupancies, for example that of *d*-orbitals in transition metals,[21] and more recently that of *f*-orbitals in lanthanides.[22] Moreover, an extension of the traditional multipole model is the spin-polarized multipole model, adding the spin-density information to the charge density.[23]

Cross-fertilized by charge-density research, ways of directly fitting the shapes of orbitals and wavefunctions to the measured diffraction pattern were also devised. This is at the heart of the original definition of quantum crystallography (QCr) given by Massa, Karle and Huang, which encompasses methods where the information resulting from traditional quantum

[1] German original: „…muß es dann gelingen, die besondere Anordnung der Elektronen im Atom experimentell festzustellen."

chemistry calculations is enhanced by external information intrinsically contained in the experimental crystallographic data.[24] The first discussion about the perspective of obtaining wavefunctions from X-ray scattering (here: Compton scattering) goes back to 1964 and the first Sagamore conference,[25,26] whereas the first quantum crystallographic method according to the original definition[24] and based on X-ray diffraction was proposed by Clinton and Massa in 1972.[27] Nowadays, Jayatilaka's X-ray constrained wavefunction (XCW) fitting approach[28-32] and its later developments[33-40] are the most popular modern versions of the original quantum crystallographic methods based on X-ray diffraction. They practically aim at determining wavefunctions that minimize the energy, while reproducing, within the limit of experimental errors, X-ray structure factor amplitudes collected experimentally. As an alternative, joint refinement methods for the complete reconstruction of N-representable one-electron density matrices exploit both X-ray diffraction and inelastic Compton scattering data. [41-43] More detailed reviews of methods can be found in reference[44] and reference[45].

In 1999, Massa, Huang and Karle also pointed out[46] that there is another stream of quantum crystallographic techniques that directly use wavefunctions and orbitals – not multipoles – to improve the accuracy and information contents of crystallographic refinements. This is basically the converse of their original definition of QCr. In this converse sense, the first developments are associated with Quantitative Convergent-Beam Electron Diffraction (QCBED)[47-50] for which the knowledge of the wavefunction describing the high-energy electron passing through the crystal is essential for solving the dynamical electron scattering equations. The solutions to these equations give the scattered intensities in calculated diffraction patterns that are compared to experimental ones in QCBED refinements. Another area in which the converse definition of QCr plays an important role is macromolecular crystallography,[51,52] where quantum mechanically derived restraints are successfully exploited to supplement the limited resolution and amount of diffraction data compared to the number of parameters needed to model atomic positions and displacements in large systems. Finally, the most recent technique in this framework is the Hirshfeld Atom Refinement (HAR),[53,54] which exploits *ad hoc* Hartree-Fock (HF) or Density Functional Theory (DFT)

computations to derive fragment electron densities for refinements that provide the most accurate and precise structural results currently attainable from X-ray data. In reference [45] both aspects of the Massa-Huang-Karle QCr definition were discussed in detail. From here on, these two aspects together are termed "original quantum crystallography".

Figure 1. The participants at the CECAM Discussion Meeting in Nancy (and co-authors of this paper) with a selection of the fields that they represent. These fields are important pillars at the outset of a discussion about a new meaning of quantum crystallography. They are not exclusive, but the starting point for a broadening of QCr.

This viewpoint paper has been initiated at the Discussion Meeting "Quantum Crystallography: Current Developments and Future Perspectives" (Nancy, France, 19-20 June 2017) under the umbrella of the European Centre for Atomic and Molecular Calculation (CECAM, Centre Européen de Calcul Atomique et Moléculaire), which was organized to discuss the meaning and perspectives of quantum crystallography in light of the recent and significant increase in the use of this term and related techniques in the scientific literature (Figure 1).[55-58] Therefore, in the following section, we will show how this increased interest in QCr manifests itself in method developments and applications that are not necessarily within the original definition of QCr or in the framework of conventional multipole-based

experimental charge density research as discussed above. In fact, if all fields and applications where quantum chemistry and experimental approaches based on diffraction and scattering mutually enrich each other are to be accommodated within a unified research area, the original definition of QCr is too narrow. In this light, in section 3 we will present and discuss the different points of view on QCr as they emerged during the recent CECAM Meeting. This will highlight different ways in which the rapid and fruitful scientific evolutions touched upon in section 2 could eventually lead to a broadened definition of quantum crystallography and to the foundation of a new and flourishing research field and community (see Figure 1).

2. Current Developments

In this section, the authors of this paper will outline current highlights from their own research activities to exemplify the wide scope of methods and applications that might be included into a broadened definition of quantum crystallography. This section can neither be an exhaustive review nor will it cover all possible areas of overlap and interest for QCr. It will show the diversity of the field, not a unified picture, so that it will pave the way for discussions about the meaning and usefulness of QCr.

In the first three subsections, we will present the two traditional ways to conduct quantum crystallographic investigations, namely the completely theoretical approach (subsection 2.1) and the completely experimental approach - the latter discussed both in terms of new technical and instrumental developments (subsection 2.2) and in terms of the traditional experimental charge density methods (subsection 2.3). We will afterwards illustrate techniques in the framework of both aspects of the original definition of quantum crystallography by introducing density-matrix- and wavefunction-based refinement strategies (subsections 2.4 and 2.5, respectively), quantum crystallographic techniques to refine crystal structures of biological macromolecules (subsection 2.6) as well as the Kernel Energy Method (KEM, subsection 2.7). We will conclude the overview of the methods of the original definition of QCr by discussing dynamic quantum crystallography (particularly the NoMoRe approach, subsection 2.8) and the quantitative convergent-beam electron diffraction

(QCBED) technique (subsection 2.9). In subsection 2.10, we will present techniques to derive information on chemical bonding from wavefunctions and electron densities. In the last five subsections, we will show how quantum crystallographic approaches are already fundamental for many interesting applications in different fields, such as in crystal engineering (subsection 2.11), in the determination of magnetic properties (subsection 2.12), in the study of molecular and extended solids (subsection 2.13), in materials science (subsection 2.14) and in crystal structure prediction (subsection 2.15).

2.1 Theoretical Quantum Crystallography

Quantum mechanical methods are one of the main ingredients of QCr. We briefly discuss here the most important approximations involved and some of the available computer codes.

Any quantum mechanical method starts with an idealization of the atomic structure. Isolated molecules can be accurately represented by a set of atomic coordinates. Solids are typically represented as perfect, infinite crystals, defined by a unit cell and a lattice, under periodic boundary conditions. However, real crystals differ from this ideal situation, due to defects, impurities, surface relaxations, non-stoichiometry, and disorder. A strength of theory is that model systems can be simulated irrespective of their existence in nature, allowing the investigation of effects associated with different modifications on system properties.

The direct solution of the many-particle Schrödinger equation is an intractable task for most systems of interest in QCr. Simplifying the electronic wavefunction to a single Slater determinant leads to the Hartree-Fock method.[59] The often severe deviation of the HF solution from the exact one is collectively termed as electron correlation. There are many so-called post-HF methods,[59] which approximate electron correlation and yield accurate many-electron wavefunctions, e.g., configuration interaction and coupled cluster methods, as sketched in Figure 2. However, the additional accuracy comes at the price of steeply increasing computational cost.

An alternative route is Density Functional Theory with the much simpler ground-state electron density $\rho(\boldsymbol{r})$ as the main variable. The ground state energy E of a system is a

functional of $\rho(\boldsymbol{r})$,[60] whose mathematical form is however unknown, thus requiring approximations. Kohn and Sham[61] (KS) proposed a scheme to make DFT calculations feasible by mapping the interacting system of electrons onto a non-interacting one that leads to the true density. The search for better DFT energy functionals is an active field of research (see, e.g., references[59,62]). The main categories of functionals are, in order of increasing complexity (see Figure 2): the Local Density Approximations (LDA),[61,63] the Generalized Gradient Approximation (GGA)[64,65] and meta-GGAs.[66] These functionals depend upon the local values of ρ, $|\nabla\rho|$, $\nabla^2\rho$ and/or τ (the kinetic energy density). It is interesting to note that these same quantities are also used in the topological analysis of the chemical bond (see section 2.10). Hybrid functionals[67] additionally include a certain fraction of HF exchange. Unfortunately, there is not a single optimal DFT functional that works well for all cases and properties. Hence, compromises are necessary. We refer the reader to a recent paper[68] critically analyzing DFT functionals in terms of accuracy and addressing their differences for molecules and solids.

There are several computer codes for molecular and solid-state quantum mechanical simulations, e.g., Quantum ESPRESSO,[69] Turbomole,[70] and WIEN2k,[62,71] implementing three very different approaches (plane waves and pseudopotentials, Gaussian basis-sets, all-electron augmented plane waves). The variety of computer codes is very useful, since each code has a different focus, but raises the issue of reproducibility of results obtained by different codes. Recently, the calculated values for the equation of states were compared using 40 different DFT method types showing that deviations between the accurate codes are smaller than those of experiments.[72] A comparison of charge densities obtained with different methods (DFT or HF-based) and different basis sets (plane waves, Gaussians) has been done in reference[73].

In summary, approximations make simulations feasible but need to be verified and improved if necessary. The combination of QM and diffraction/scattering experiments within QCr is certainly a promising route for future progress in this field. For example, there are numerous examples that demonstrate that experiments guided by QM are often the only way to an

unambiguous atomic structure determination of low-dimensional systems.[74] As a further example, the usage of modern non-local functionals coupled with molecular dynamics has allowed to interpret experimental results in molecular crystals at finite temperature.[75]

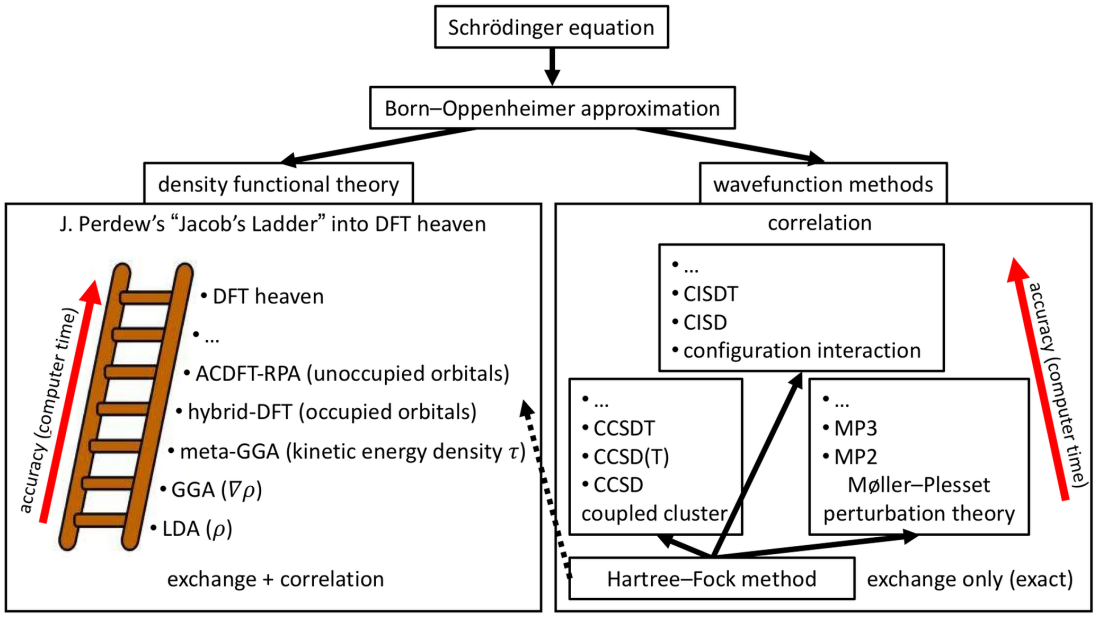

Figure 2. The most important quantum mechanical approximations and methods. The many-particle Schrödinger equation is simplified using the Born-Oppenheimer approximation. From there, one route is DFT and the other is the HF method. The most important post-HF methods that approximate electron correlation missing in HF are based on Coupled Cluster (CC) and Configuration Interaction (CI) techniques as well as the Møller–Plesset (MP) perturbation theory.

2.2 Development of experimental techniques and instruments

Outstanding data quality is required for performing a traditional multipole refinement[15] or an X-ray Wavefunction Refinement (XWR)[76]. In addition to highest quality crystals, a high-end experimental setup is the key to extracting a meaningful crystallographic outcome.

Coupled to multilayer X-ray optics, high-brilliance microfocus sealed tubes[77] and rotating anode sources dramatically increase the available X-ray flux density in comparison to conventional sealed tubes, a major benefit in the field of experimental charge density research. Data collection times can thereby be reduced from weeks to days/hours and weakly diffracting samples can now be studied more easily. Modern short-wavelength sources (Ag/In Kα) extend the data resolution limit and minimize X-ray absorption and extinction. In

parallel, large-scale facilities (synchrotrons) are becoming more widely accessible. Properties like the extraordinary X-ray flux and a tunable wavelength make them attractive, although "only a minor fraction of the published electron density literature" data is collected there.[78] This may seem surprising but is explained with the fact that there is no dedicated charge density beam line satisfying the special requirements to collect high-quality charge density data.[77]

Alongside source development, major accomplishments in the field of X-ray detection have been achieved. Today's HPADs (Hybrid Pixel Array Detector) and CPADs (Charge Integrating Pixel Array Detector) are detectors based on Complementary Metal-Oxide-Semiconductor (CMOS) technology and these are capable of fast shutterless data collection. This removes significant sources of errors such as read-out overhead, shutter jitter and goniometer repositioning inaccuracies. The HPAD technology is presently the standard technology at protein synchrotron end stations. Such detectors are known for their sensitivity, high speed, and dynamic range. However, HPADs do have limitations for charge density experiments. Strong low-resolution reflections, which contain the bonding electron density information, may suffer from count-rate saturation[79] and charge-sharing effects can lead to information loss. [78,80,81]

The appearance of X-ray Free Electron Laser (XFEL) facilities led to the development of CPADs to overcome these limitations.[82] The high-frequency readout and mixed mode operation, combining the advantages of integration for strong signals with the photon counting approach for weak signals, recently became available for the home laboratory. Although CPADs have excellent count-rate linearity, they can suffer from pixel saturation, leading to missing reflections. Sophisticated data-scaling programs aid to ensure data completeness by handling different frame exposure times or different primary beam intensities (e.g. beam attenuation).[83]

Besides sources and detectors, precise multi-axis goniometers allow the collection of true data multiplicity and keep the crystal scattering volume as constant as possible. Together with rigid sample mounts, this is a key to data quality.

Sophisticated software is necessary to accurately process the carefully collected frames. Images measured with a scan width significantly smaller than the crystal mosaicity are beneficial for data quality when using modern detectors.[84] Up-to-date integration routines apply an incident-angle correction, which takes the X-ray conversion factors of the individual detector into account.[85] Absorption and Lorentz/Polarization corrections as well as scaling, the latter being particularly important for Gaussian-shaped beam profiles, guarantee high data quality.[86] Some programs even offer a dedicated charge density mode,[82] which, among other functionalities, prevents data bias introduced by standard structure error-model settings.[87]

In conclusion, an impressive number of recent technological innovations support the scientists to successfully determine charge-density distributions. The on-going collaboration between researchers, hardware and software providers will drive future developments from which the QCr community, as well as the entire single-crystal X-ray diffraction community, will benefit.

2.3 Charge Density from X-ray diffraction

The charge density of a crystal is a quantum mechanical observable in an X-ray diffraction experiment. In principle, Fourier summation of measured structure factors should provide direct access to experimental electron densities. In practice, it is necessary to use a model of the charge density to minimize consequences of the lack of structure factor phases, experimental errors and finite resolution.

The most widely used Stewart-Hansen-Coppens multipole model[15,88] relies on the observation that spherically-averaged free-atom electron densities provide a very good zero-th order approximation of the electron density of a crystal (and a molecule). The multipole model consists of atomic electron densities, which are pre-computed from first-principles of quantum mechanics at a high level of theory. The spherical atomic cores are supplemented with additional pre-defined radial functions, which are combined with spherical harmonics to account for the asphericity of the atomic electron density. Only selected parameters of the multipole model are allowed to vary. Traditionally these are populations and expansions/contractions of valence electron densities. More recently,[89] the corresponding

parameters of core densities were allowed to change as well.

The model, starting from free quantum-physical atoms, allows to 'measure' the response of $\rho(\boldsymbol{r})$ to the formation of molecules (chemical bonds),[90] supramolecular assemblies[91] and crystals,[92] and to other physical stimuli, such as different temperatures,[93] high pressure,[94] light[95] or possibly an external electric field.[96,97] Parameters of the multipole model are usually refined by a least-squares fitting against experimental observations. Thus, first principles of quantum mechanics are not imposed during this process, as they are in the case of quantum mechanical computations. Therefore, the wavefunction is not a result of a multipole refinement and information contained in the experimental data alone should guarantee that the obtained model obeys first principles. Nevertheless, the multipole model can provide a charge density model as good as a double-zeta basis-set representation, is mature and its application is fast. Moreover, unlike in X-ray wavefunction refinement,[98] the extracted experimental information can be easily identified and the danger to "get what you put in" is smaller ("in data we trust"[99]).

With the ever-rising quality of experimental data, more and more fine details of the electron density are observed with the help of the multipole model: chemical bonds, lone pairs, crystal field effects on electron density of transition metals,[100] core region contraction upon chemical bond formation,[89] intermolecular charge transfer [101] and electron density polarization upon interaction with neighboring molecules.[92] In addition, the model provides the means to observe a high degree of transferability of atoms in similar chemical environments and to build pseudoatoms databanks. [102-105]

Therefore, the multipole model allows to study many quantum phenomena, and to obtain a predominantly experimental answer to research questions that depend on $\rho(\boldsymbol{r})$. However, as with any other model, care must be taken not to interpret the model beyond its limits[106] and not to ask for information absent in the experimental data.[107] An example of a suitable research question is measuring the correct covalent bond distance from X-ray diffraction in bonds involving hydrogen atoms. Here the multipole model permitted to get a better answer than the IAM early on,[105,107] in rather close agreement to HAR.[108,109] More recently, the

bond distance of hydrogen in the vicinity of a metal atom was characterized.[110] The power of the multipole model is also illustrated by research that aims at understanding interactions in macromolecular complexes of biological importance. Here the model provides fast access to electrostatic potential, electrostatic energies and the topology of $\rho(\boldsymbol{r})$,[111,112] while still maintaining the accuracy of quantum mechanical computations.[113,114]

2.4 Density matrix refinement and data combination

To this day, quantum crystallography mostly relies on the interplay between spin or charge densities derived from first-principles calculations and X-ray Diffraction (XRD) or high-resolution Polarized Neutron Diffraction (PND) experimental data. Despite their high quality and the absence of extinction effects, few studies have made sole use of QCBED-derived structure factors to reconstruct charge densities (see Introduction and Subsection 2.9). Their number is usually small and a full reconstruction process necessitates complementing them with higher-Q Fourier components obtained by "traditional" X-ray methods.[115,116] This is a clear example of the need of combining two experimental data sets to take the best of what is available experimentally. As explained in Subsection 2.12, the problem is found to be rather similar in the spin density case, although the limitations are not as stringent as those encountered in the QCBED technique.[117] However, when such difficulties are circumvented, electron density reconstruction is still not a (spin resolved) wavefunction extraction.

The work carried out on electron spin density can be somewhat extended by considering the reduced density matrix formalism. Obviously, no *N*-electron wavefunction has yet been recovered this way, but significant advances can be (and have been) made, including the possibility of tackling the problem from a phase-space perspective. In its simplest expression, the one-electron reduced density matrix (1-RDM), which was strongly promoted by Weyrich or Massa and co-workers during the 1980s and 1990s,[118-121] can be seen as the most direct object to connect position and momentum space properties[122] and thereby offers an efficient means to combine XRD, QCBED and PND data with experimental results provided by inelastic scattering techniques, such as polarized or non-polarized X-ray Compton, gamma-e-

gamma scattering or positron annihilation.[123] Moyal or Wigner functions (see, for example, reference[124]), could equally be considered to play the same role. The pure state 1-RDM $\rho(\boldsymbol{r},\boldsymbol{r}')$ is associated with the N-electron wavefunction from:

$$\rho_k(\boldsymbol{r},\boldsymbol{r}') = \int \psi_k^*(\boldsymbol{r},\boldsymbol{r}_2,\ldots,\boldsymbol{r}_N)\,\psi_k(\boldsymbol{r}',\boldsymbol{r}_2,\ldots,\boldsymbol{r}_N)\,d\boldsymbol{r}_2\ldots d\boldsymbol{r}_N \qquad (1).$$

This puts rather strong constraints on the form taken by experimentally derived 1-RDMs which are required to be *N*-representable (see also Subsection 2.7) and, in the pure-state case, idempotent $\int \rho_k(\boldsymbol{r},\boldsymbol{r}'')\,\rho_k(\boldsymbol{r}'',\boldsymbol{r}')d\boldsymbol{r}'' = \rho_k(\boldsymbol{r},\boldsymbol{r}')$. Nevertheless, no such condition can be imposed on experimentally derived 1-RDMs, which are expected to originate from a mixture of states and expressed by means of each microstate canonical probability p_k,

$$\rho_k(\boldsymbol{r},\boldsymbol{r}') = \rho_\uparrow(\boldsymbol{r},\boldsymbol{r}') + \rho_\downarrow(\boldsymbol{r},\boldsymbol{r}') = \sum_k p_k\rho_k(\boldsymbol{r},\boldsymbol{r}') \qquad (2),$$

where the spin up and down contributions have been made explicit. For data from XRD, PND, non-polarized Compton Scattering (CS) and Magnetic Compton Scattering (MCS), the spin-resolved 1-RDM, for a given scattering vector $\boldsymbol{g}$, is connected to structure factors through

$$F_{XRD}(\boldsymbol{g}) = \int \left(\rho_\uparrow(\boldsymbol{r},\boldsymbol{r}) + \rho_\downarrow(\boldsymbol{r},\boldsymbol{r})\right) e^{-i2\pi\boldsymbol{g}\cdot\boldsymbol{r}}d\boldsymbol{r} \qquad (3)$$

and

$$F_{PND}(\boldsymbol{g}) = \int \left(\rho_\uparrow(\boldsymbol{r},\boldsymbol{r}) - \rho_\downarrow(\boldsymbol{r},\boldsymbol{r})\right) e^{-i2\pi\boldsymbol{g}\cdot\boldsymbol{r}}d\boldsymbol{r} \qquad (4)$$

and, for Compton profiles in a scattering direction given by $\boldsymbol{u}$, through

$$J_{CS}(q,\boldsymbol{u}) = \int \left(\rho_\uparrow(\boldsymbol{r},\boldsymbol{r}') + \rho_\downarrow(\boldsymbol{r},\boldsymbol{r}')\right) e^{-i\boldsymbol{p}\cdot(\boldsymbol{r}-\boldsymbol{r}')/\hbar}\delta(\boldsymbol{p}\cdot\boldsymbol{u}-q)d\boldsymbol{r}\,d\boldsymbol{r}'d\boldsymbol{p} \qquad (5)$$

and

$$J_{MCS}(q,\boldsymbol{u}) = \int \left(\rho_\uparrow(\boldsymbol{r},\boldsymbol{r}') - \rho_\downarrow(\boldsymbol{r},\boldsymbol{r}')\right) e^{-i\boldsymbol{p}\cdot(\boldsymbol{r}-\boldsymbol{r}')/\hbar}\delta(\boldsymbol{p}\cdot\boldsymbol{u}-q)d\boldsymbol{r}\,d\boldsymbol{r}'d\boldsymbol{p} \qquad (6).$$

These equations demonstrate the importance of density matrix determination of experimental quantities derived from scattering techniques, which are at the very heart of crystallography. Results provided by coherent elastic scattering of X-rays, polarized neutrons, polarized X-

rays and electrons are related to the Fourier coefficients of the electron or spin density in crystals, hence the diagonal elements of the density matrix (see equations (3) and (4)). Conversely, spectra from X-ray incoherent inelastic scattering, as well as spectroscopic methods, such as positron annihilation or e-gamma-e, dominantly address the off-diagonal part of the same 1-RDM (see equations (5) and (6)). Therefore, the 1-RDM, as the simplest and closest transcription of a wavefunction, but adapted to mixed state configurations, can be considered as a common denominator of a large range of experimental techniques, making it possible to check their mutual coherence.

While the refinement of 1-RDM models can still be considered as a very recent research field, the past decade has witnessed strong advances thanks to the fruitful joint efforts of theoreticians and experimentalists with respective expertise in scattering techniques as complementary as high resolution XRD, PND, CS and MCS. An example of a tentative 1-RDM reconstruction from pseudo-data is given in Figure 3.

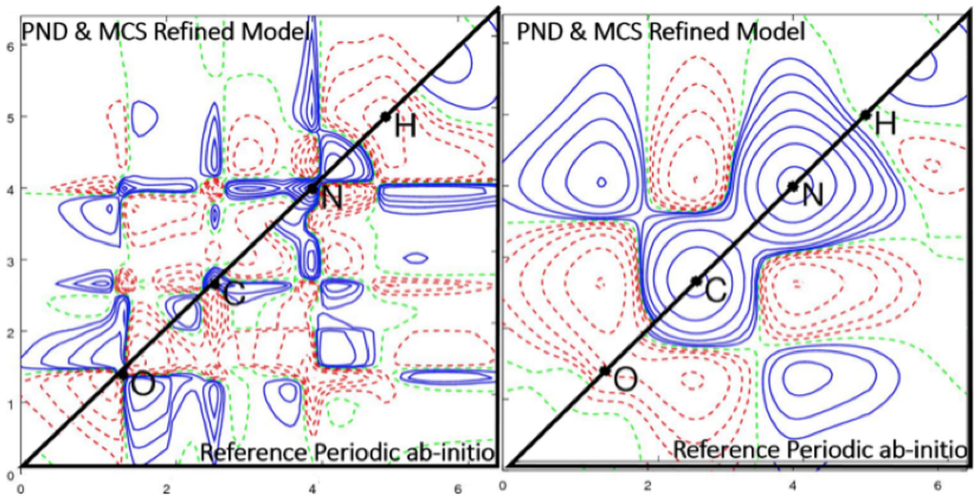

Figure 3. Refined 1-RDM for the toy model triplet-state urea in a periodic lattice with parallel molecules separated by 3 Å. Left: a path through O, C, N and H in the molecular plane. Right: a similar path but 0.5 Å above the plane. The upper half is the refined 1-RDM for a simple single molecule model (expressed on a 3-21G(d) basis set). The lower half represents the reference result, namely a periodic DFT computation with an extended basis-set (pob-TZVP), from which 12 MCS profiles and 500 PND structure factors were computed and used for the refinement.[125]

2.5 Wavefunction-based refinement

The wavefunction is the fundamental entity that intrinsically contains all the information about a system. Therefore, there is a direct relationship between the structure factors of X-ray or electron diffraction – the Fourier transforms of the electron density – and the wavefunction. With modern computing power and increasing experimental accuracy, this relationship can be exploited more and more efficiently for crystallographic refinement.

On the one hand, the already mentioned X-ray constrained wavefunction fitting approach[28-32] (see introduction) plays a prominent role. It was initially developed in the framework of the Restricted Hartree-Fock formalism[28,29,31] and was afterwards extended to other approaches (e.g., Density Functional Theory,[32] relativistic Hamiltonians,[33,34] Extremely Localized Molecular Orbitals (ELMOs),[35-38] etc.). Several investigations have shown that XCW fitting allows not only to obtain reliable charge density distributions, but also to determine physical properties of materials[126-129] (e.g., non-linear optical properties) and to consistently capture electron correlation,[130] polarization and crystal field effects. Other exciting ongoing studies also focus on the capability of the method in capturing relativistic effects[34] and in reliably determining experimental spin densities for interesting open-shell systems, such as the cyclic alkylaminocarbene radical cAAC-$SiCl_3$,[131] for which preliminary results are available.

From the methodological point of view, future challenges for the technique are its extensions to periodic systems and to multi-determinant wavefunction approaches, although the recent X-ray Constrained ELMO-Valence Bond (XC-ELMO-VB) method[39,40] can be already considered an attempt in the latter direction.

On the other hand, tailor-made wavefunctions have already been successfully used to improve X-ray structure refinements by means of HAR.[53,54] In its current implementation, molecular electron densities are theoretically calculated and afterwards partitioned using Hirshfeld's stockholder partitioning method.[132,133] This enables a "classical" atom-centered crystallographic description and a least-squares refinement of atomic positions and thermal parameters using quantum atoms. These contain all the information from the parent wavefunction (or electron density) from which they have been partitioned. The HAR procedure is iteratively repeated until convergence is reached. Recent investigations have

revealed that HAR currently provides the most accurate and precise structural results from X-ray data, even for the positions of hydrogen atoms.[108,109,134] A future challenge for HAR is the need of extending its applicability to large molecules (e.g., proteins) and to heavy-metal systems (e.g., coordination compounds). Coupling HAR with *ab initio* linear-scaling strategies (e.g., techniques based on the transferability of ELMOs[135,136]) would allow considerable progress in this respect.

Finally, an intriguing future perspective in this framework is the systematic coupling of the two approaches discussed above (i.e., XCW fitting and HAR) to give rise to what has been termed X-ray Wavefunction Refinement.[98] A thorough validation of XWR has recently been conducted and showed that the new approach can indeed be considered as a method for both structure and charge density determination from experiment.[76]

2.6 Quantum refinement of biological molecules

Quantum refinement is a method to supplement standard crystallographic refinement with quantum mechanical calculations.[51,52,137,138] In the refinement process, the model is optimized to provide an ideal fit to the experimental raw data (the structure factors).[139] For resolutions obtained for most biological macromolecules, 1–3 Å, available data are not numerous enough to determine the exact positions of all atoms. Therefore, as a first attempt, the experimental data were supplemented by empirical chemical information in the form of a Molecular Mechanics (MM) force field. Consequently, the refinement takes the form of a minimization of the function:[139]

$$E_{\mathrm{cryst}} = E_{X-ray} + w_{\mathrm{A}} E_{\mathrm{MM}} \quad (7)$$

where w_{A} is a weight factor that is required because the crystallographic ($E_{\mathrm{X-ray}}$) and MM (E_{MM}) energy functions do not have the same units.

This works fairly well for proteins and nucleic acids, for which there are plenty of information about the ideal geometry so that a MM description works well.[139] However, for other parts of the structure, e.g. metal sites, substrates, inhibitors, cofactors and ligands, such

information is normally missing or much less accurate. Moreover, the MM description is rather inaccurate, omitting electrostatics, polarization and charge transfer. This can be solved by employing a more accurate energy function, provided by QM calculations, which involve all energy terms and do not require any parameterization.[51,52,137,138] In the first implementation of this quantum-refinement approach, QM was employed for a small, but interesting part of the macromolecule, using the energy function[51,137]

$$E_{\mathrm{QM-refine}} = E_{\mathrm{X-ray12}} + w_{\mathrm{A}}\left(E_{\mathrm{QM1}} + E_{\mathrm{MM12}} - E_{\mathrm{MM1}}\right) \quad (8)$$

where E_{QM1} is the QM energy and the subscripts indicate whether the method is used for the whole macromolecule (12) or only for the QM region (1).

This approach was implemented in 2002 using DFT calculations.[51,137] It was shown to locally improve the geometry of metal sites in proteins.[140] Moreover, the protonation state of metal-bound ligands could be determined by comparing quantum-refined structures optimized in different protonation states using real-space *R* factors and comparing geometries and energies with those obtained for the QM system in vacuum.[141] In the same way, the oxidation state of metal sites could be deduced, although it often changes during data collection, owing to photoreduction by electrons released in the crystals by the X-rays.[142,143]

In 2004, a related approach was presented, in which a linear-scaling semiempirical QM method was employed for the entire protein, obtained by simply replacing E_{MM} in Equation 7 by E_{QM}.[52,138] It was shown that the re-refinement could correct structural anomalies in the original refinement of a 1 Å-resolution protein structure. This approach has later been extended to other software, including also QM/MM and *ab initio* methods.[52,138,144]

Quantum refinement has been applied to many systems of biological or chemical interest, e.g. heme proteins, zinc proteins, superoxide dismutase, hydrogenase and nitrogenase.[51,52,137,138,141-143,145-149] Typical applications regard the nature, protonation and oxidation state of the active site, comparing different structural alternatives, as shown in Figure 4. Applications to drug design and ligand refinement[144,150-155] have advanced the accuracy of the determination of small-molecule parameters in active site pockets over what

is possible with standard models, in which the ligand force-field is generally less well validated than that for the protein. Naturally, the largest effects are typically seen for low resolutions and at resolutions better than ~1 Å, effects of systematic errors in the QM method start to be apparent. The method has been extended to neutron,[156] NMR[157-163] and EXAFS (Extended X-ray Absorption Fine Structure) refinement.[164-168]

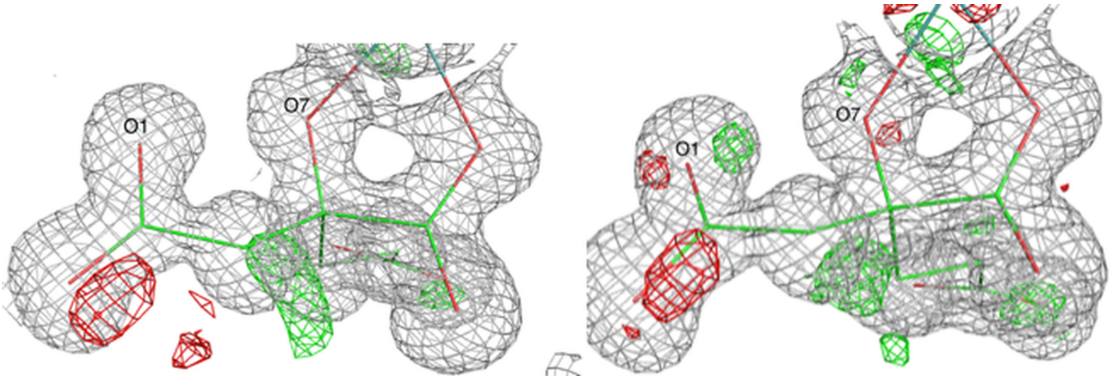

Figure 4. Electron-density maps of two possible protonation states of the homocitrate ligand in nitrogenase.[149] The $2mF_o - DF_c$ maps are contoured at 1.0 σ and the $mF_o - DF_c$ maps are contoured at +3.0 σ (green) and –3.0 σ (red). The structure to the left fits the experimental data better, especially around the O1 and O7 atoms. This is also reflected by the real-space difference density Z-scores, which are 3.0 and 3.2, respectively. Reprinted with permission from reference[149] (Copyright 2017 American Chemical Society).

2.7 X-ray diffraction and N-representability

The compliance with the *N*-representability is a *sine qua non* to obtain quantum mechanically rigorous density matrices from X-ray diffraction data. In this context, the conversion of X-ray diffraction data into an electron density matrix $\rho(\boldsymbol{r},\boldsymbol{r}') = Tr\boldsymbol{P}\,\boldsymbol{\psi}(\boldsymbol{r})\boldsymbol{\psi}(\boldsymbol{r}')$ (where $\boldsymbol{P}$ is a population matrix and $\boldsymbol{\psi}$ is a column-vector collection of atomic basis functions) that reflects the antisymmetry of an *N*-electron wavefunction is accomplished by applying iterative Clinton matrix equations[169] of the form:

$$\boldsymbol{P}_{n+1} = 3\boldsymbol{P}_n^2 - 2\boldsymbol{P}_n^3 + \sum_k \lambda_k^{(n)}\,\boldsymbol{O}_k \qquad (9)$$

where $-\lambda_k^{(n)}$ is the k-th Lagrangian multiplier pertaining to enforcement of an X-ray scattering observable represented by the matrix $\mathbf{O}_k$.

Figure 5 pictures all antisymmetric wavefunctions and all *N*-representable 1-body density matrices. Given a valid wavefunction, by integration over its square, one obtains a quantum mechanically satisfactory density matrix. In general, an arbitrary 1-body function $f(\boldsymbol{r},\boldsymbol{r}')$ will not map back to the set of valid antisymmetric wavefunctions. However, beginning with an *N*-representable density matrix, this will map back to a wavefunction, which defines it as *N*-representable.

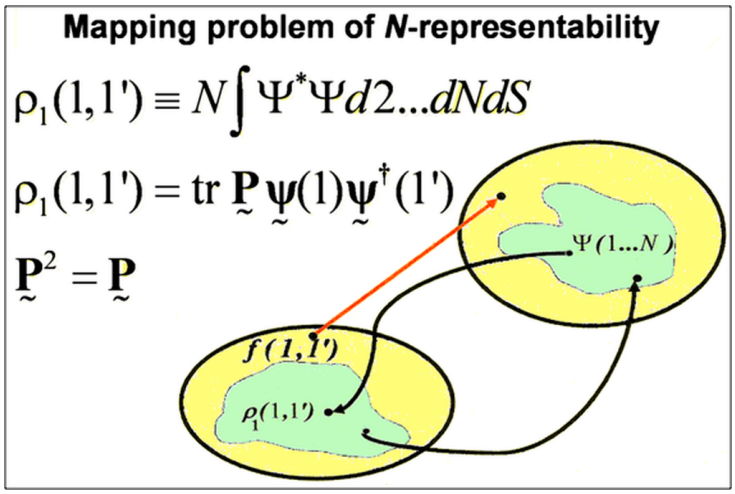

Figure 5. Sketch depicting the mapping problem associated with wavefunction *N*-representability of density matrices.[170]

For single determinant *N*-representability, the density matrix shall be a projector, *i.e.*, $\boldsymbol{P}^2 = \boldsymbol{P}$, encompassing that of Density Functional Theory solutions of the Kohn-Sham equations. Walter Kohn was fond of saying that "…the only purpose of the KS orbitals is to deliver the exact density". In this regard, one may take notice that orbitals of the experimental X-ray determined density matrix of form $\boldsymbol{P}^2 = \boldsymbol{P}$ do just that.

This would be satisfactory and deliver a complete quantum mechanics for small organic molecules containing a few tens of atoms. However, this would not work for biological molecules containing very large numbers of atoms, N_{at}. That is because the number of unknowns grows more rapidly with increasing N_{at} than does the number of experimental data. To surmount the difficulty arising from insufficient data one may invoke the Born-

Oppenheimer approximation, using nuclear positions obtained from crystallography, and then, instead of an experimental fit, theoretically calculating the density matrices. Nevertheless, at this point the problem is that the difficulty of quantum chemical calculations rises as a high power of the number of atoms.

The Kernel Energy Method (KEM) is a successful way of calculating the *ab initio* density matrices for molecules of any size. KEM was devised by Massa, Huang and Karle[24] based upon previous work related to the Clinton equations and it has been thoroughly tested against a wide variety of biological molecules and also extended aromatics with and without imposed strong external electric fields.

The KEM working equation for the total energy is,

$$E_{\substack{total \\ (KEM)}} = \sum_{a=1}^{m-1} \sum_{b=a+1}^{m} E_{ab} - (m-2) \sum_{c=1}^{m} E_c \quad (10)$$

and the corresponding KEM density matrices are

$$\rho_2 = \sum_{a=1}^{m-1} \sum_{b=a+1}^{m} \rho_{2ab} - (m-2) \sum_{c=1}^{m} \rho_{2c} \quad (11),$$

$$\rho_1 = \sum_{a=1}^{m-1} \sum_{b=a+1}^{m} \rho_{1ab} - (m-2) \sum_{c=1}^{m} \rho_{1c} \quad (12),$$

$$\rho = \sum_{a=1}^{m-1} \sum_{b=a+1}^{m} \rho_{ab} - (m-2) \sum_{c=1}^{m} \rho_c \quad (13).$$

In the above equations, E_{ab} is the energy of a double kernel of name *ab*, E_c is the energy of a single kernel of name *c*, ρ_2, ρ_1, ρ symbolize respectively, two-body density matrices, one-body density matrices and electron densities.

Notice that the QCr/KEM procedure extracts the complete quantum mechanics based on the X-ray experiment. However, there is no mathematical requirement that the KEM summation of kernels must be *N*-representable. Again, to resolve this QCr/KEM shortcoming, the Clinton equations will prove to be sufficient (see for example illustrations in reference[171]).

Summarizing, the importance of the Clinton equations within QCr/KEM means that true

quantum mechanics can be extracted based on X-ray data (this in KEM form) and then made to be guaranteed single Slater determinant *N*-representable. This paragraph emphasizes discussion of the complete quantum mechanics in single determinant form, for both small and large molecules, a close experimental analogy to the theoretical single determinant form of DFT.

2.8 Dynamic Quantum Crystallography

A plethora of important bulk solid-state properties depend on crystal vibrational properties. The atomic and molecular motions determine the vibrational entropy of crystals, and are therefore crucial for understanding stabilities and phase changes. Mechanical properties, such as the elastic moduli of the crystal, are also intrinsically linked to the crystal lattice dynamics. Information on the correlation of atomic motion is lost in the standard elastic scattering experiment. However, the atomic motion gives rise to changes in the diffraction intensities, which are taken into account in the form of the Debye-Waller factor. The temporal and spatial average of the atomic fluctuations - mean square displacements - can therefore be retrieved from a diffraction measurement, and in recent work this information has been combined with lattice-dynamical models derived from periodic DFT calculations.[172,173] In this approach, the amplitudes of the acoustic and lowest-frequency optical phonons are refined against the diffraction intensities. In the simplest model, these phonon modes are approximated by the motion at the Gamma point of the Brillouin zone.

Despite the very simple lattice dynamical model, these Normal Mode Refinements (NoMoRe) capture essential information about the crystal dynamics from the experiment. In Figure 6 the heat capacity of naphthalene obtained from calorimetric measurements is compared with the heat capacities obtained by the NoMoRe procedure, as well as with the related models of Bürgi and Aree.[174]

The atomic mean square displacements obtained by fitting the normal modes against the diffraction intensities compare well with the displacements obtained from standard crystallographic models. Additionally, the hydrogen atom anisotropic displacements compare

well with independent information from neutron diffraction experiments. However, by combining aspherical atom refinement and normal mode refinement, it is evident that there is information in the diffraction experiments that is not captured by the model;[175] there is plenty of room for improvements. One obvious next step in quantum crystallographic studies of dynamics is to model Thermal Diffuse Scattering (TDS).

Studies of diffuse scattering from crystals are experiencing a renaissance in these years. This is due to the advent of very sensitive low-noise detectors and because high-performance computing has made it possible to construct *ab initio* models of crystals that can explain diffuse patterns. Diffuse scattering patterns originate from ordering at length scales larger than the unit cell dimensions. The ordering can be of either static or dynamic character, and in both cases, it reveals important information about the physical properties of the crystal.

The TDS signal can be diminished by cooling the crystals to very low temperatures, but it can never be fully removed. If TDS is not accounted for it will give rise to additional systematic changes in the Bragg intensities, and thus create artifacts in the crystallographic models, as it was recently demonstrated in a model study on silicon and cubic boron nitride.[176] This implies that even in quantum crystallographic studies where the dynamics is of secondary interest, it is important to have an accurate model of motion in order to properly take these contributions into account.

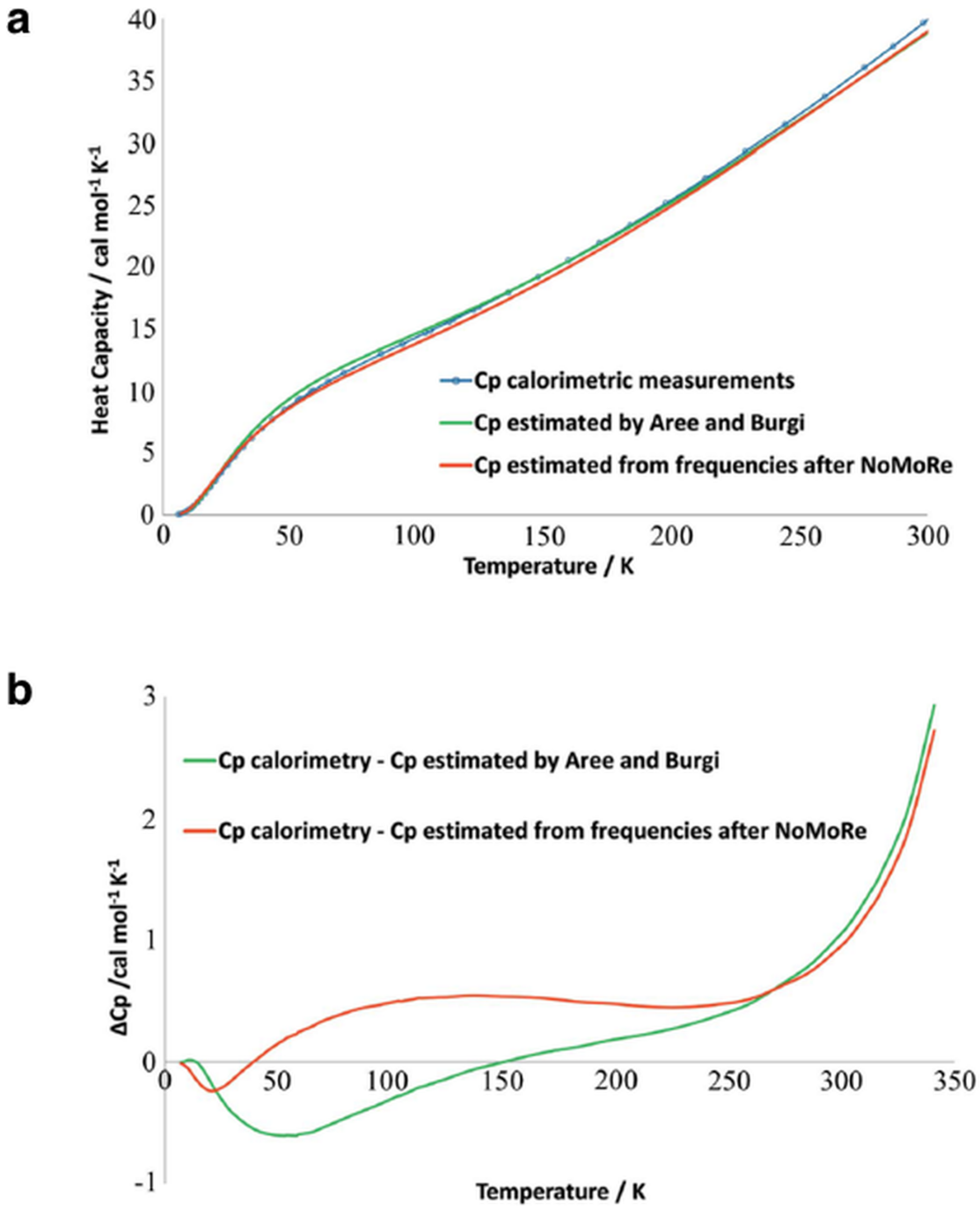

Figure 6. (a) Heat capacity (Cp) of naphthalene: from thermodynamic measurements (blue curve), calculated from frequencies obtained after NoMoRe (red curve) and estimated by Aree and Bürgi (green curve), (b) difference between Cp from calorimetric measurements and Cp estimated by Aree and Bürgi (green curve) and from NoMoRe (red curve). Reprinted from reference[173] under the general license agreement of IUCr journals.

2.9 Electron density from quantitative convergent-beam electron diffraction

The electron density, $\rho(\boldsymbol{r})$, and the electrostatic potential, $V(\boldsymbol{r})$, at position $\boldsymbol{r}$ within a crystal can be described by the following Fourier sums:

$$\rho(\mathbf{r}) = \frac{1}{\Omega}\sum_{\mathbf{g}} F_{\mathbf{g}}\ e^{-i2\pi\mathbf{g}\cdot\mathbf{r}} \quad (14)$$

and

$$V(\mathbf{r}) = \sum_{\mathbf{g}} V_{\mathbf{g}}\ e^{-i2\pi\mathbf{g}\cdot\mathbf{r}} \quad (15).$$

The sums are over reciprocal lattice vectors $\mathbf{g}$, Ω is the unit cell volume, and $F_{\mathbf{g}}$ and $V_{\mathbf{g}}$ are the Fourier coefficients (structure factors) of the electron density and crystal potential, respectively. By applying Poisson's equation in relating charge distribution to electrostatic potential, the Mott formula[177] describes the relationship between $F_{\mathbf{g}}$ and $V_{\mathbf{g}}$ as follows:

$$F_{\mathbf{g}} = \sum_j Z_j e^{-2\pi i\mathbf{g}\cdot\boldsymbol{r}}\, e^{-B_j s^2} - V_{\mathbf{g}}\left(\frac{16\pi^2\varepsilon_0\Omega s^2}{|e|}\right) \quad (16).$$

The sum is over all atoms, j, in the unit cell with atomic numbers Z_j and Debye-Waller factors B_j and positions $\boldsymbol{r_j}$. The free-space permittivity is ε_0, $|e|$ is the magnitude of the electronic charge and $s = (sin\theta)/\lambda$.

In X-ray diffraction experiments, $F_{\mathbf{g}}$ are the observables because X-rays interact with the electron distribution, whilst in electron diffraction, $V_{\mathbf{g}}$ are the observables because electrons, being charged, interact with the crystal potential. From equations 14-16, it is evident that X-ray and electron diffraction measure quantum mechanically valid features of crystals, namely the electron distribution and the electrostatic potential. They are, therefore, complementary techniques in quantum crystallography.

Electrons, being charged, can be focused into nanometer-sized (or smaller) probes using electromagnetic lenses in standard electron microscopes. Additionally, the position of the focal point within the specimen can be controlled (using electromagnetic deflection) with sub-nanometer precision. Due to their charge, electrons interact about 10^4 times more strongly

with matter than X-rays and specimens must therefore be very thin (~100 nm) in order to avoid strong absorption. This high spatial confinement and selectivity means that Convergent-Beam Electron Diffraction (CBED) patterns can be obtained from regions of perfect crystallinity, avoiding grain boundaries, dislocations, stacking faults, voids, surface blemishes and other imperfections.

The technique of Quantitative Convergent-Beam Electron Diffraction (QCBED) involves the matching of a simulated CBED pattern to an experimental one whilst varying the structure factors of reflections at or near the Bragg condition, V_{hkl} (i.e. $V_{\mathbf{g}}$), and the specimen thickness, H, to optimise the fit. Over the last three decades, QCBED has developed to where it can routinely measure bonding-sensitive low-order structure factors with uncertainties of the order of 0.1%.[178-186] Furthermore, it can do so without extinction and scale problems because the analysis uses a full dynamical treatment of electron scattering, necessitated by the strong interaction of electrons with matter. Figure 7 schematically illustrates QCBED from data collection to the determination of a deformation electron density. From the refined values of the structure factors given in the caption, the very high level of precision within such a refinement is evident.

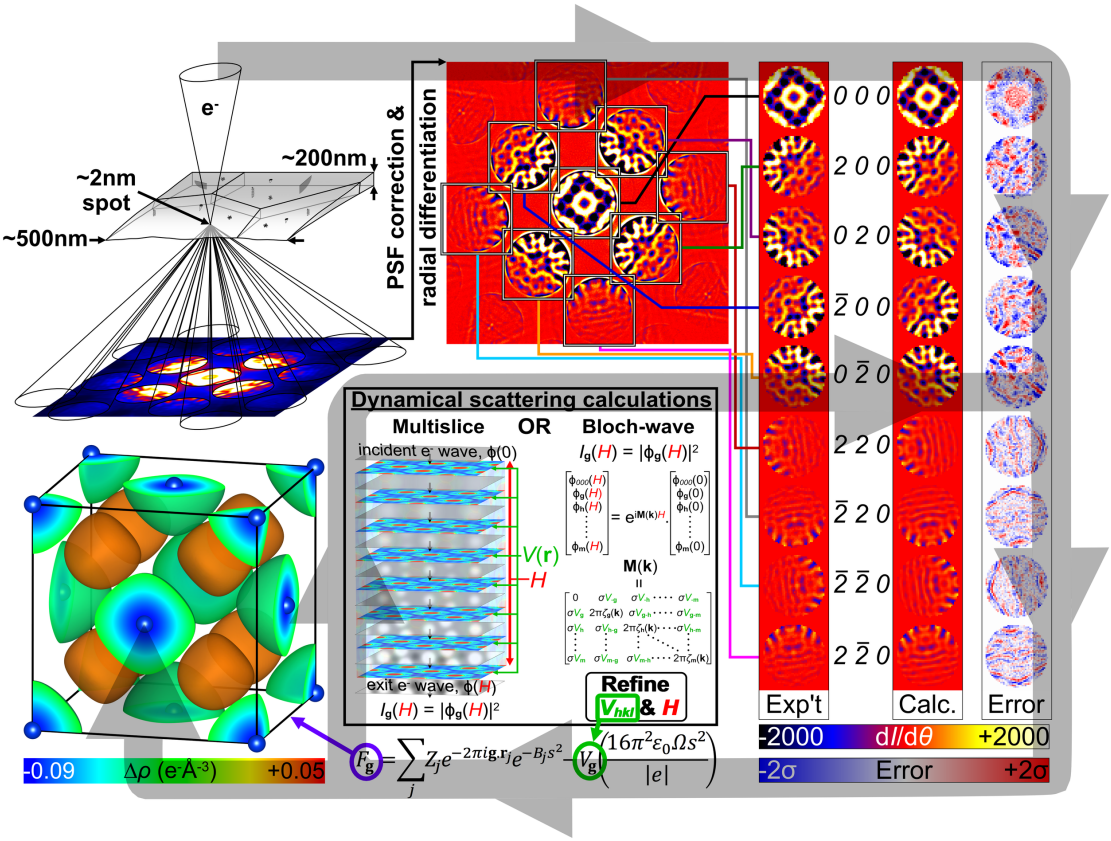

Figure 7: A summary of QCBED. The first step is CBED data collection from a region of perfect crystal (~10^{-25} m^3 in volume). Very high spatial selectivity makes it easy to avoid crystal imperfections and surface blemishes. The CBED patterns are corrected for instrumental point spread function[187] (PSF) and are differentiated to remove the inelastic background.[185,188] Selected reflections are pattern matched with full dynamical electron scattering calculations using either the multislice[189] or Bloch-wave[190,191] formalisms. The structure factors of reflections at or near the Bragg condition, V_{hkl} or $V_{\mathbf{g}}$, and the crystal thickness, H, are refined to minimize the mismatch (following the loop of the grey arrow). The refined $V_{\mathbf{g}}$ can be converted to $F_{\boldsymbol{g}}$ via the Mott formula[177] for the determination of the deformation electron density, $\Delta\rho(\boldsymbol{r})$, as shown here for the example of aluminium[186] (drawn with *VESTA*[192]). In this example, the CBED pattern was collected with 160 keV electrons along [001]. The refined structure factors were V_{200} = 5.29±0.01 V (F_{200} = 33.39±0.03 e^-) and V_{220} = 3.219±0.006 V (F_{220} = 29.35±0.04 e^-) at T=0K. The refined specimen thickness at the electron probe position was H = 1056±1 Å.

2.10 Chemical bonding analysis

A pillar of the emerging field of quantum crystallography is represented by the group of methods aiming at analyzing the chemical information contained in experimental and theoretical static electron density distributions. Quantum Chemical Topology (QCT) does so

by analyzing local functions, *f*, which yield a chemical picture of the system:

$$f: \mathbf{R}^3 \text{ (molecular space)} \rightarrow \mathbf{R} \text{ (chemical picture)}$$

These methods are epitomized by Bader's Quantum Theory of Atoms in Molecules (QTAIM)[193] whose departing function is the electron density, $f = \rho(\boldsymbol{r})$. The existence of a bond is associated with the presence of a first-order Critical Point (CP) in the electron density (or Bond Critical Point, BCP) and of the gradient line joining it to the linked atoms (or Bond Path, BP).[194] Figure 8 shows the ability of bond paths to reveal both covalent and intermolecular interactions in a benzene crystal. QTAIM, through integrations over atomic basins, yields atomic properties such as QTAIM charges (carbon and hydrogen charges, q, shown in Figure 8), atomic multipoles and volumes. The examination of BCPs provides insight into the structure and stability of crystals revealed in the bonding patterns that can be obtained from either theoretical or experimental electron densities.[195]

Localization and delocalization (sharing) indices have also been defined within QTAIM by integrals of the Fermi hole density (or exchange-correlation hole density in correlated calculations). Delocalization indices δ can yield insight on the driver of the binding between monomers of a dimer, whether "through bond" or "through space" (*i.e.*, non-bonded atoms)[196] (see Figures 8 and 9). This information can be condensed in matrix format known as the Localization-Delocalization Matrix (LDM).[197] LDMs are of fundamental interest but also have practical applications in Quantitative Structure-Activity Relationship (QSAR) predictions of molecular properties.[197,198] LDMs need the first- and second-order density matrices for their construction, which for experimental densities requires the techniques introduced in the previous sections. Thus, generally at the time of writing, when only the electron density is available, then LDMs cannot be calculated from the experimental data alone. However, a complete population analysis including localization and delocalization information can be derived from the Laplacian of the electron density, an experimentally accessible quantity, from the Bader-Gatti Source Function (SF)[199] which can also be casted in a matrix form and used in a similar fashion as LDMs.[200]

Due to their delocalized nature, special *f* functions have been designed to visualize non-covalent interactions. As an example, the reduced density gradient (aka NCI for Non Covalent Interactions)[201] has been designed to detect weak interactions such as halogen bonds from the electron density. It helps to provide more stable pictures that do not change upon the quality of X-ray refinement.[202] Weak interactions in a benzene crystal are shown within this approach in Figure 8. The delocalized nature of CH-π vs CH-C interactions is apparent.

Another important set of *f* functions are those for the analysis of electron pairing, such as the electron density Laplacian,[203] the Electron Localization Function (ELF)[204] and the Electron Localizability Indicator (ELI).[205] This family of functions identifies localized electrons, such as those in covalent bonds and lone pairs (Figure 8). By integration over bonds and lone pairs, properties (e.g. valence populations as shown in Figure 8) can be obtained. This analysis allows for example to rationalize the formation of channels in MOFs, clathrates or molecular crystals.[206] It is important to note that the ELF and ELI require the first-order density matrix, so that quantum crystallography developments also hold great potential for these analyses.[57]

f	QTAIM	NCI	ELF	LDM
Image	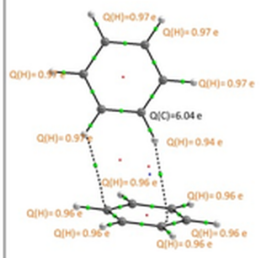	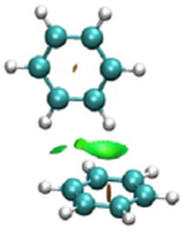	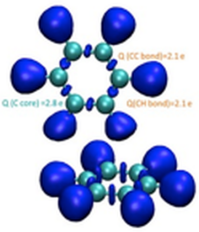	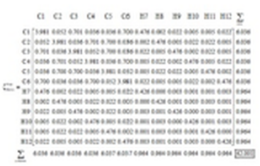
Reveals	Atoms and bond paths summarized at points	Weak interactions	Localized electrons (bonds, lone pairs)	Delocalization among all atom pairs
Needs	Electron density		1st order RDM	2nd order RDM

Figure 8. CH-π and CH-C interactions in a benzene crystal: (a) QTAIM, (b) NCI, (c) ELF. (d) LDM for isolated benzene (see Figure 9 for LDM of the benzene dimer).

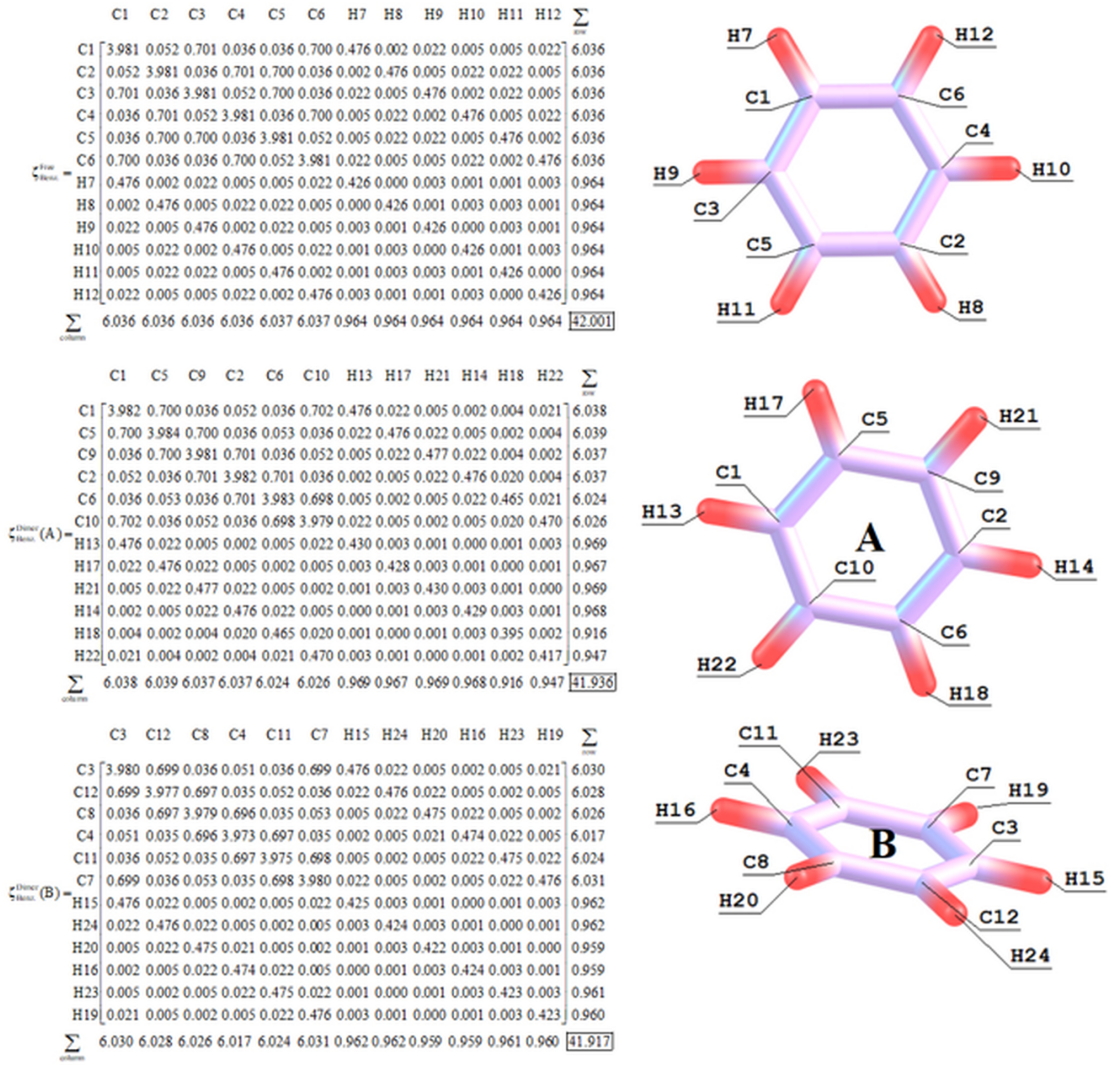

Figure 9. (*Top*) Localization-Delocalization Matrix of an isolated benzene molecule, and (*middle and bottom*) the two partial LDMs (sub-matrices) of monomers A and B of a benzene dimer (without the 2x12x12 interaction elements that appear in the full 24x24 matrix of the dimer). Note that the sum of column or rows of the isolated benzene molecule is 42.001 indicating a +0.001 cumulative integration error (numerical noise), which is 0.002% of the exact electron population of benzene (N = 42). The full 24x24 LDM of the dimer (not shown) sum to 83.996 (with a cumulative integration of -0.004). The difference between that total dimer population (that includes the numerical noise) and the sum of the populations of monomers A (41.936) and B (41.917) within the dimer is 0.143 electrons. Those 0.143 electrons are delocalized between the two rings and hold them together, taking as the most dominant delocalization bridges the atoms connected by inter-monomer bond paths, namely, $\delta(\mathrm{C4,H22}) = 0.02$, $\delta(\mathrm{C12,H18}) = 0.01$, but also other atoms mainly $\delta(\mathrm{C4,C10}) = 0.01$, and $\delta(\mathrm{C7,H18}) = 0.01$.

2.11 Crystal Engineering

Molecular recognition, molecular assembling and molecular organization in space are three of the most important aspects in the study of intermolecular interactions. They have a strong impact in large domains of science such as crystal growth, crystal engineering, supramolecular chemistry and materials science, because the physical-chemical properties of supramolecular entities and crystalline solids do not only depend on the molecules they are constituted of, but also on the way molecules interact with each other. This is a straightforward consequence of the structure-properties relationship. The case of polymorphism in crystalline solids can be invoked as an example of the modification of the solid properties induced by different organizations of the same molecules in space. The variability that these molecules can display in their assembling can thus be understood in terms of the several possibilities existing in the recognition between different molecular regions.

From the Hellmann-Feynman theorem,[207,208] the electron density distribution $\rho(\boldsymbol{r})$ in the ground state of any molecular system only depends on the nuclear positions. Accordingly, $\rho(\boldsymbol{r})$ is straightforwardly related to the molecular structure, because the latter is defined by the atomic positions that are in turn identified by those of the nuclei. On the other hand, the Hohenberg & Kohn theorem[60] states that the total energy of a system can be written in terms of its electron density distribution. Hence, bringing together both fundamental theorems, the $\rho(\boldsymbol{r})$ function emerges as a conceptual bridge between the structure and the energetic properties of molecular systems. A good strategy to understand the relationship between them is thus the analysis of $\rho(\boldsymbol{r})$, which codes essential features of the molecular organization in space because it reflects the molecular interactions in the system. By extension, these features are not only implicitly coded in $\rho(\boldsymbol{r})$, but also in its derived properties, as in the Laplacian $\nabla^2\rho(\boldsymbol{r})$ and the electrostatic potential *V(r)*. These scalar functions characterize the regions of the space where $\rho(\boldsymbol{r})$ is locally concentrated ($\nabla^2\rho(\boldsymbol{r}) < 0$) or depleted ($\nabla^2\rho(\boldsymbol{r}) > 0$) and the molecular electrophilic ($V(\boldsymbol{r}) > 0$) and nucleophilic ($V(\boldsymbol{r}) < 0$) regions.

The topological analysis of any scalar function provides richer information than appears from the direct observation of the function itself. In the widely used QTAIM theory,[193] this kind of analysis has been deeply developed for $\rho(\boldsymbol{r})$ to characterize many aspects that this function exhibits in atoms, molecules and their interactions. As an alternative, analogous topological concepts to $\nabla^2\rho(\boldsymbol{r})$ and $V(\boldsymbol{r})$ can be applied to get insights into recognition, assembling and organization of molecules in space. Hence, the study of the topological critical points (CP) of $\nabla^2\rho(\boldsymbol{r})$ has indicated that charge concentration (CC) and charge depletion (CD) sites found in the valence shell of atoms are driving geometric preferences of molecules in the solid state.[209-211] This is shown in Figure 10a, where directional nucleophilic-electrophilic interactions between several CC and CD sites are simultaneously involved in the relative orientation of three molecules in a crystal. Additionally, specific CPs along bonding directions point out the nature of interactions.[212,213] Thus, in the polyiodide chains of the crystal structure of tyrosinium polyiodide hydrate (Figure 10b), iodines are distinguished from iodides by the type of CPs found in their interactions with surrounding atoms. In the case of $V(\boldsymbol{r})$, its gradient vector field (*i.e.* the electric field $\epsilon(\boldsymbol{r}) = -\nabla V(\boldsymbol{r})$) and the corresponding zero-flux surfaces originating from its topology permit to characterize the force lines driving the early interaction between molecules and the extension of the influence zones that molecular electrophilic and nucleophilic sites exhibit in intermolecular regions (Figure 10c).[214] Furthermore, the intersection of the gradient vector fields of $\rho(\boldsymbol{r})$ and $V(\boldsymbol{r})$ has shown to bring the elements for the understanding of the counterintuitive assembling of anion-anion and cation-cation aggregates,[215-218] pointing out the regions of space that are involved in local attractive electrostatic interactions in hydrogen[219] and halogen[212] bonding. To illustrate these features, Figure 10d shows the phosphate-phosphate aggregation at equilibrium geometry, where attractive electrostatic forces take place in the hydrogen-bonding region and keep the complex assembled. Indeed, in spite of the global destabilizing interaction due to Coulombic repulsion (interaction energy > +100 kJ/mol), the system is

trapped in a sharp potential well and ~70 kJ/mol are needed to overcome the energetic barrier to dissociate the aggregation.

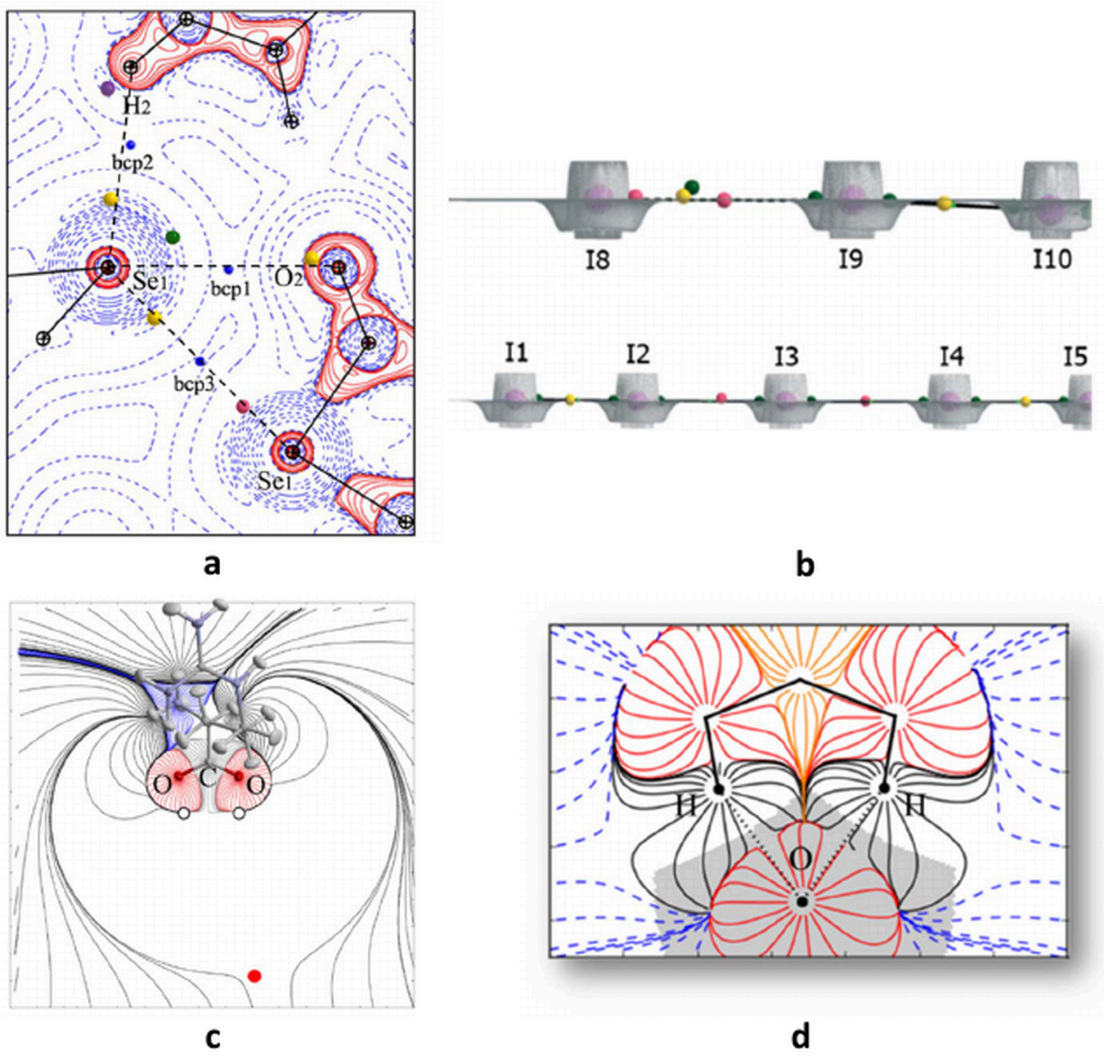

Figure 10. (a) $L(\boldsymbol{r}) = -\nabla^2\rho(\boldsymbol{r})$ experimental map in intermolecular regions of the $C_8O_2H_4Se$ crystal structure: CC sites are represented by (3,-3) CPs of *L* (yellow spheres), CD sites are denoted by (3,+3) (violet), (3,+1) (pink) and (3,-1) (green) CPs of *L*. CC…CD directions closely correspond to internuclear directions (dashed lines), which in turn almost superimpose with bond path directions (bond critical points are in blue). (b) CPs of $L(\boldsymbol{r}) = -\nabla^2\rho(\boldsymbol{r})$ in two regions of a poly-iodide chain (same color-code used in (a)): covalent bonds are identified by (3,-3) CPs in the middle of the bonds of I1-I2, I4-I5 and I9-I10, while intermolecular interactions are characterized by (3,+1) CPs in the middle of I2…I3…I4 and I8…I9 regions. I9 is an iodine atom making a type-II halogen bonding interaction with iodine I8 (I8(CC)…(CD)I9) and a covalent interaction with I10, whereas I3 is an iodide displaying non-covalent interactions with both I2 and I4 iodine. (c) Experimental gradient vector field of $V(\boldsymbol{r})$ for the L-histidinium cation in the crystal structure of L-histidinium phosphate phosphoric acid: the influence zone of its nucleophilic COO-group is limited by a zero-flux surface of $V(\boldsymbol{r})$, the distance up to the saddle point in the surface ((3,+1)

CP, red sphere) being approximately 6 Å. (d) At the equilibrium geometry of the phosphate…phosphate complex, the O-atomic basin (grey region) lays within the influence zones (electrostatic basins) of the H-nuclei. Black $\epsilon(\boldsymbol{r})$ lines crossing the region between the zero flux surfaces of $\rho(\boldsymbol{r})$ (grey border) and $V(\boldsymbol{r})$ (red lines border) are attractive force lines, whereas blue $\epsilon(\boldsymbol{r})$ dashed-lines crossing the same region are repulsive force lines. Figure 10a reprinted with permission from reference[211], Copyright 2013 American Chemical Society; Figure 10b reproduced from reference[212] with permission from the Royal Society of Chemistry; Figure 10c reprinted with permission from reference[214], Copyright 2007 American Chemical Society; Figure 10d is adapted from Figure 3 (upper left, including atomic labels) in reference[216], Copyright 2013, with permission from Elsevier.

2.12 Spin Densities

Modeling magnetic properties of crystalline compounds by experiments is a challenging task for many reasons. First, the electrons contributing to the magnetism are few compared to the overall content of the unit cell. A second problem comes from the necessity of obtaining good quality crystals of suitable size for neutron diffraction (mm^3) supporting high irradiation and longtime data collection. Finally, the magnetic properties usually appear at very low temperature (helium cooling) and experiments require magnetic fields to be applied on the samples, excluding routine experiments. At the end, the number and the experimental resolution of the collected data are limited, allowing to refine models with only a limited number of parameters.

Recently, new methodological routes and software have being developed combining data obtained by different techniques such as X-ray and polarized neutron diffraction[23,220] or polarized neutron and X-ray magnetic diffraction.[221] Combining different experiments is a way to overcome limited resolution and leads to more precise models of spin or spin-resolved electron densities. From these joint refinements, experimental charge density or wavefunction-based models can be obtained. These experimental models are of utmost importance to test high-level theoretical calculations, as recently shown for a paramagnetic radical.[117]

To analyze these modeled (or theoretical) spin densities, new methods are developed or adapted, thus giving rise to new tools to explore magnetic pathways in crystals. For example, the Source Function method can produce representations that allow for visualization of the magnetic pathways and for conclusions about the specific role played by each atom along them.[222]

Another complementary way is to combine theoretical calculations and experimental data sets in constrained wavefunction refinement approaches.[28-30,32] This method has proven to be efficient for combining X ray data and calculations, but one can imagine to include in this approach experimental magnetic structure factors.

All these promising developments should not mask several critical aspects. First, neutron diffraction facilities are undergoing significant changes: most reactors will close (ILL in Grenoble, LLB in Saclay), but spallation sources appeared around the world (Switzerland, Japan, USA…) and a new one is under construction in Sweden (ESS, Lund) for the European researchers. These new facilities should develop beam-lines able to carry out polarized neutron diffraction experiments (like MAGIC at ESS), but also ensure our community with a sufficient beamtime access. To support this demand, we have to enlarge the number of possible users of our methods and this represents the second important point. For this, we have to consider that, until now, the studied crystals are mainly organic or metal-organic compounds. To open our community to solid-state physicists, we have to apply our methods to inorganic compounds in order to prove their capabilities in exploring the magnetic properties of these materials. A possible approach consists in including delocalized electrons in our models. Indeed, experimental Compton and magnetic Compton profiles can be used to model delocalized spin and charge densities that are of fundamental importance in inorganic material (for example, in conducting properties studies). Proposing this kind of new and more complete model is a currently ongoing effort.[223]

2.13 Molecular & Extended Solids

Molecular and extended solids (M&ES) include quite diverse objects: on the one hand molecular crystals made by organic, inorganic or metallorganic molecules and, on the other hand, extended systems formed by *n*-dimensional (*n*=1-3) periodic networks, such as ionic solids (salts), covalent/polar solids (*e.g.* semiconductors; binary compounds: carbides, silicides, nitrides, ...) and metallic, intermetallic and low-dimensional organometallic compounds. Focus here is only on the non-organic M&ES, although some of the exposed considerations apply equally to the organic M&ES in specific cases.

Most M&ES are of relevance for their technological applications and are intensely scrutinized, with QCr playing a basic role in the puzzle that relates their geometrical structure, chemical bonding nature and properties to each other.

A common trait of many M&ES is that the sole knowledge of their crystal structure is not enough to infer their chemical and electronic structure.[195,224,225] Chemists always like to draw dashes, arrows and dotted lines connecting atoms or groups of them, but there are plenty of M&ES where this operation is ambiguous or simply impossible, if based on their structure alone. Electron density and wavefunction analyses are often used to provide insights. Nevertheless, even with these tools, the answer may not be unique, as it may depend on the kind of descriptor that is used and on the physical space with which such descriptor is associated (1-electron $\rightarrow R^3$, 2-electrons $\rightarrow R^6$, basis-function space, local or non local, *etc*.).[224]

There are M&ES in which two or more alternative pairs of atoms compete for a bond path and where even a negligible change of geometry leads to an abrupt change in the crystal graph (which is the entirety of the bond paths in the crystal). Description in terms of topology is sharply *discontinuous* in such a case, while it is *continuous* in terms of electron sharing between pairs of atoms, regardless of a bond path linking them exists or does not exist.[224] This impasse, partly solved by showing that BPs play the role of privileged electron exchange channels,[226] has called for an ever increasing adoption of continuous descriptors, directly/indirectly related to electron pairing and able to characterize multi-center bonding as

well as the strengthening or weakening of competing interactions in series of chemically related systems.[224] The delocalization indices (DI),[196,227,228] the ELF,[229] the ELIs,[230] the Domain Averaged Fermi Hole (DAFH), [231,232] the Source Function[233] and the descriptors inherent to the Interacting Quantum Atom (IQA)[230] energy decomposition supply a non exhaustive list of them. Their joint use provides complementary, often compelling insight, but warrants thoughtful analyses.[195,224] Apart from the Source Function, all these descriptors require the pair density or at least the 1-RDM for their evaluation, calling for QCr tools to retrieve them directly from *ab initio* methods or, indirectly, through the XCW approach. Although akin to an orbital picture, DAFH analysis is fully derived from a quantum observable. It so establishes a link with the localised single-particle states approaches (ELMOs,[234] Natural Bond Orbitals (NBOs)[235], extremely localized Wannier functions[236]).

Besides defining the network of bonds, QCT methods serve for characterizing their nature. When heavy atoms are involved, the task is not as simple as for bonds within light elements.[195,224] It calls for additional descriptors to be examined[237] and/or conventional ones to be reinterpreted.[195,224]

Many properties of M&ES, like those related to electronic transport, depend directly on reciprocal space properties (*e.g.* energy dispersion of electronic bands in *k*-space). Yet, not much is known on how the characteristic features in the band structure are reflected in the electron density.[238] This relevant, although seldom explored QCr aspect, has been tackled in a study on transition metal carbides[238] and for optimizing thermoelectric compounds *via* orbital engineering.[239]

M&ES provide an endless field of application and development for QCr approaches. Figure 11 details two examples.

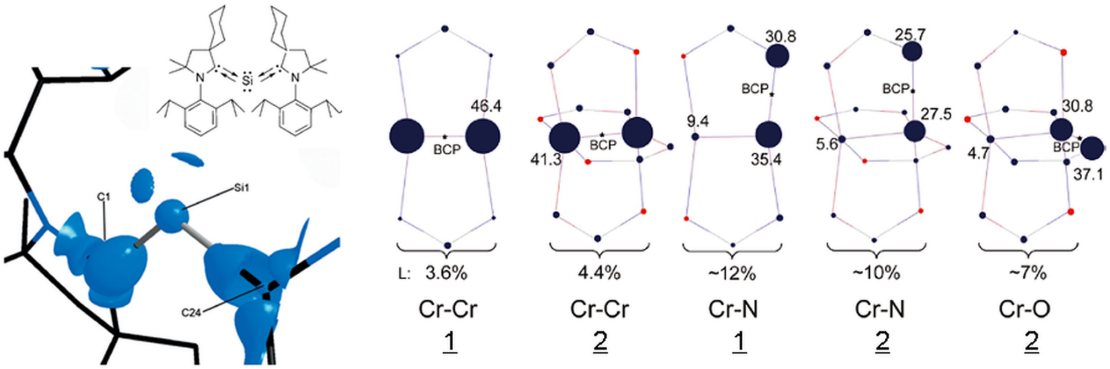

Figure 11. Examples of application of QCr methods to the realm of molecular and extended solids. (*Left*) Two separated valence shell charge concentrations, indicative of two lone pairs, are present in the non-bonding region of the central Si atom. They confirm the interpretation of the compound $(cAAC)_2Si$ as a silylone stabilized by two cyclic alkyl amino carbenes (experimental electron density Laplacian isosurfaces, $\nabla^2\rho$ = -2.5 eÅ^{-5}). Adjusted from Scheme 1 and Figure 1 with permission from reference[240], Copyright 2014 Wiley-VCH Verlag GmbH & Co. KGaA, Weinheim. (*Right*) A combined experimental and theoretical charge density study on the quintuply bonded dichromium complex (**1**) $Cr_2(dipp)_2$ (dipp = (Ar)NC(H)N(Ar) and Ar = 2,6-*i*-Pr_2 -C_6H_3) The electron density at the Cr-Cr BCP is essentially determined by the metal ions, as shown by the Source Function percentage (SF%) contributions [contrast SF% values for Cr-Cr and Cr-X (X=N,O) interactions]. Blue and red balls indicate sources and sinks, respectively. Data for compound **2** with formal bond order 4 are reported for the sake of comparison. Adjusted from Figure 8 with permission from reference[241], Copyright 2011 American Chemical Society.

2.14 Quantum Crystallography and Materials Science

Although quantum mechanics may appear as a complicated theory that is understandable only to experts in the field, a huge array of recent inventions rely on it (opto-electronic components, devices to store and transform energies, thermoelectric materials, etc.). Even if many phenomena were known also in the pre-quantum mechanics era, only after its development one could correctly interpret the mechanisms and therefore design materials, beyond models based on classical mechanics. Nonetheless, the quantum mechanical information extracted from experiments remains largely unused, and this is true in crystallography as well. However, the recent research in quantum crystallography opens new perspectives and potential applications, as described in the following.

Quantum magnets are appealing materials, consisting of spin centers coupled through exchange interactions. They may give rise to extended networks of different dimensionality as well as to zero dimension molecular magnets. Superconducting quantum interference or muon spin spectroscopy are methods to measure magnetic susceptibility, spatial ordering and spin dynamics, and thereafter derive simple models of exchange. However, the quantum information is limited to the spin states and their relative energies, whereas scattering experiments, in particular elastic or inelastic neutron diffraction, enable to model the magnetic structure of a crystal and its dynamics. Moreover, flipping ratios measurements[242] of polarized neutron diffraction allow the refinement of spin density distributions in solids,[243,244] even in combination with the charge density, as recently demonstrated.[23] The charge and spin density models inform on the electron correlation, the preferential exchange paths and the corresponding strength of spin coupling. This is vital to understand how the magnetism works and how to optimize the material design.[245]

Dielectric properties are equally important in materials science. The industry of semiconductors seeks for high- or low-dielectric constant materials (with respect to SiO_2), necessary for the miniaturization of micro-electronic components, to reduce the size of gate dielectrics or to guarantee better separation between transistors.[246] In telecommunication industry, transparent materials with high refractive index are fundamental to improve the performances of fiber optics.[247] The direct observation of atomic and molecular polarizations, due to the internal electric fields in crystal, is a clue of the atomic/molecular polarizability. Spackman and Jayatilaka[126] demonstrated the possibility of calculating polarizabilities of molecules in crystals using X-ray constrained molecular orbital calculations. Using the quantum theory of atoms in molecules, one can calculate polarizabilities of atoms, functional groups or molecules embedded in crystalline matrices and therefore recognize key factors for the technological requests.[248]

Quantum crystallographic approaches also enable the characterization of non-equilibrium phenomena in molecular crystals, due to photo-excitation or X-ray probe pulses.[249] Because these phenomena depend on structural changes on a wide time scale, time-resolved

experiments (down to femtosecond resolution) are essential to understand processes that underlie material behaviors. Although experimental requirements do not yet allow a very accurate mapping of the charge density, one may envisage a fruitful synergy between theoretical approaches and experimental measurements to overcome current limitations.

Quantum crystallographic studies on many other kinds of materials, such as thermoelectric pulses, metals and alloys, superconductors etc.,[250] have appeared with the goal of finding a more robust structure-property correlation. The advanced methodologies of quantum crystallography may certainly enable to gain more insights into the nature of properties.

2.15 Crystal Structure Prediction

Crystal Structure Prediction (CSP) was an almost impossible challenge for a long time,[251,252] but recent methodological developments[253] have eventually made CSP manageable and led to many successes and impressive discoveries. [254-257] Given a chemical formula, CSP stands for finding the corresponding stable crystal structure at a given pressure (and temperature). A simultaneous prediction of all stable stoichiometries and structures for a set of composing elements is performed using the variable-composition variant of CSP methods.[258]

CSP is a global optimization problem since the stable structure is associated with the lowest minimum of the free energy surface.[253] The starting point in metadynamics, simulated annealing, basin hopping, and minima hopping approaches is chosen in a good region of configuration space to avoid sampling in poor regions, while in the self-improving methods the best structures are located step by step, using evolutionary algorithms. The latter are particularly suited and powerful for CSP, being unbiased, fully *ab initio* (only the exact or variable chemical composition need to be known) and able to produce, by their own nature, increasingly good structures in subsequent generations.[258]

Intimate relationships link CSP and QCr. An enthalpy or free energy value needs to be computed for each sampled structure in CSP approaches. Depending on the method, also a local structural relaxation is derived using quantum mechanical (periodic electronic structure)

calculations or suitable force fields, calibrated *via* QM calculations. DFT approaches are generally adopted, but they have their well-known limits - a tendency to prefer electron delocalization (HF methods behave oppositely)[259] favoring delocalized metal-like structures over covalently bonded insulating structures. In addition DFT has the difficulty in properly evaluating dispersion energy effects with a uniform accuracy in the whole range of sampled pressures.[260,261] Therefore predicted structures and phase diagrams need to be validated[254-257] through experiments, also inherently related to QCr (X-ray diffraction, Raman spectroscopy, *etc*.).

CSP often involves exploring unbeaten tracks of potential energy surfaces, leading to the discovery of new structures where a totally new chemistry emerges, with exotic, unanticipated bonding situations. [254-257,262,263] Indeed, even at moderate pressure (< 10 GPa), the compressive energy, which adds up to the system internal energy, is akin to the energy of a moderate strength hydrogen bond and, at high pressure (<100 GPa), is large enough to break normal chemical bonds.[262] Our usual chemical knowledge is based on the periodicity of atomic properties (radii), reflecting the periodicity in the electron configurations of the outermost shell. When pressure increases, the variation in atomic radii across the periodic table becomes much less important and thus, *e.g.*, the distinction between alkali and transition elements progressively vanishes.[262] For a study of chemical bonding in such unconventional cases, this requires completely unbiased approaches, such as the Quantum Chemical Topology methods,[264] based on QM observables, the heart of QCr.

One representative example is the recent discovery[256] of Na_2He, the first neutral thermodynamically stable compound of He (at pressure > 113 GPa), using a variable-composition evolutionary CSP approach, followed by experimental validation and rationalization of its geometrical and electronic structures in terms of QCT methods (Figure 12). Na was loaded into a He medium in a laser-heated diamond anvil cell and compressed up to 155 GPa, with synchrotron X-ray diffraction used to monitor sample evolution. Na_2He resembles a 3D checkerboard with Na_8 cubes alternatively filled with He or allocating an interstitially localized electron pair, revealed by a non-nuclear attractor electron density

maximum and a massive accumulation in the deformation electron density map. Na_2He is an electride, with localized electron pairs forming 8-center-2-electron bonds within the empty Na_8 cubes.

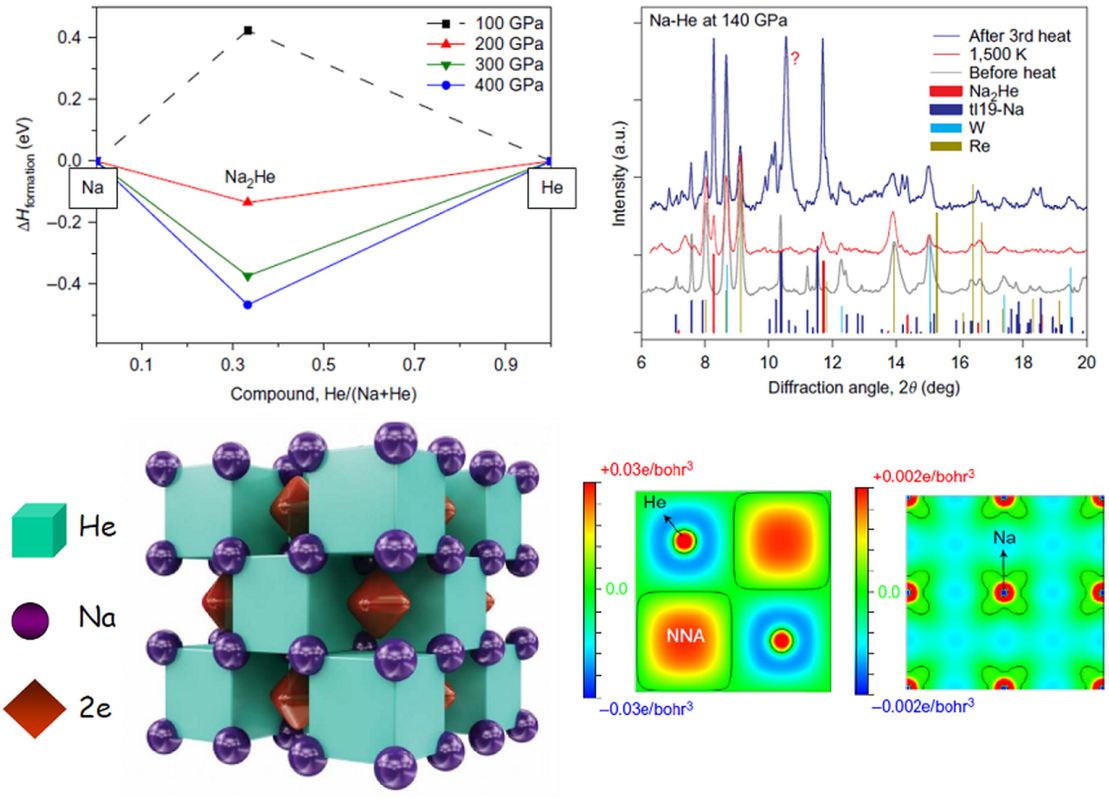

Figure 12. Na_2He: (*Top left*): predicted convex hulls of the Na-He system, based on the theoretical ground states of Na and He at each pressure. The calculated $\Delta H_{formation}(Na_xHe_{1-x}) = xH(Na) + (1-x)H(He) - H(Na_xHe_{1-x})$ (H = enthalpy) indicates that Na_2He has a lower enthalpy, hence is thermodynamically more stable, than the mixture of elemental Na and He, or any other mixture, at pressures above 160 GPa. (*Top right*): Synchrotron XRD data. Below 113 GPa only single crystal reflections of elemental Na were observed, whereas above this pressure new single crystal reflections appeared, which became even stronger after laser heating to a temperature > 1500 K. Vertical ticks correspond to expected positions and intensities of XRD peaks of Na_2He, tI19-Na, Re (gasket) and W (pressure gauge). (*Bottom left*): Geometric and electronic structure of Na_2He. (*Bottom right*): Interaction density in the (100) plane of Na_2He passing through He atoms. This quantity was obtained by making separate calculations on the Na and He sublattices (i.e. Na_2He without He and without Na, respectively) and subtracting the resulting electron densities from that of Na_2He. NNAs indicate interstitial electron localizations. Insertion of He pushes electron density out, causing its interstitial localization. Adjusted from Figures 1, 3 and 4 with permission from reference[256] and (bottom right) from Figure 1 in reference[265], with permission from and credit to Artem Oganov, Skolkovo Institute, Moscow, Russia.

3. Future Perspectives

In the previous sections, it emerged that significant research based on quantum mechanics encompasses several areas of crystallography, both experimental and theoretical, with a strong interplay between them. This implies the existence of a field of quantum crystallography, although a concise and comprehensive definition is difficult, at least at this stage. Thus, the question remains: what exactly is quantum crystallography?

According to Feynman,[266] quantum mechanics "is the description of the behavior of matter and light in all its details and, in particular, of the happenings on an atomic scale". Among various fields, he mentioned also the study of periodically arranged quantum systems. Often scientists use "quantum mechanics" and "quantum physics" as synonyms, to emphasize the intrinsic quantum nature of all investigations dealing with atoms and molecules. For this reason, in physics, quantum mechanics is not a purely theoretical discipline, but it embraces all aspects of a natural science: *observations*, *rationalizations*, *theorizations* and *applications*. On the contrary, quantum chemistry and quantum biology, although lacking of a formal definition, are often perceived only as theoretical disciplines that provide answers by performing computer calculations and exploiting sophisticated software. Nevertheless, both of them have experimental counterparts, mainly spectroscopy or any form of energy conversion. On the other hand, quantum crystallography is more naturally bound to scattering experiments, as clearly reflected in the original definition by Massa, Karle and Huang,[24,46] as well as in many previous works on refinements of electron densities, density matrices and wavefunctions.[6,14,15,27,28,88] In fact, historically, the interplay between quantum mechanical models and experimental scattering data has been enormous and vital for crystallography in its entirety (see Introduction).

We want to highlight that, in general, the term "quantum" does not only refer to computational approaches. In fact, experiments by themselves can reveal the quantum nature of matter and describe quantum mechanical phenomena (e.g. the Stern-Gerlach experiment, Bose-Einstein condensation, superconductivity, tunneling effects, or, in fact, scattering of X-rays by electrons and of electrons by the electric potential). In turn, crystallography, being a

natural science, is not only associated with observations (and not only with scattering techniques). Quantum mechanical models have always been necessary to interpret the measurements and overcome the loss of the phase information in the X-ray diffraction data. Furthermore, crystallography also consists of direct applications of first-principle quantum mechanical methods with periodic boundary conditions (nowadays implemented in world-wide recognized software, such as Quantum Espresso,[69] WIEN2k, [62,71] Crystal,[267] VASP,[268-271] Turbomole[70]) to solve problems in solid-state physics/chemistry.

Nevertheless, while the original definition of QCr encompasses only the developments and applications of strategies that combine quantum mechanics and experimental scattering in a strictly intertwined protocol, it is evident that other facets of quantum crystallography foster a broadening of its definition. In the following subsections, we present the different perspectives that have emerged so far and their possible implications.

I. First option: Preserving the original meaning

According to this view, quantum crystallography would remain tightly linked to wavefunction or density matrix modeling with constraints to scattering experiments and, conversely, to the improvement of crystallographic information via *ad hoc* QM calculations. In this option, the purpose of QCr is making predictions of crystal features and properties more reliable than from pure first-principle calculations or experimentally derived models. An advantage of this option is that a clear definition is possible that coincides with the historic development of the term, thus avoiding misunderstandings. One relevant drawback of this vision is the exclusion of charge density refinements, which exploit the more traditional multipole model techniques or the maximum entropy method.

II. Second Option: Outcome-based definitions.

Option 1 clearly limits QCr to the instrumental scope of enhancing quantum mechanical models or crystallographic information through their suitable combination, when, actually, information on a system may also be enhanced the other way around. A different definition

could indeed be based on the purpose of the study, without a rigid limitation to experimentally constrained wavefunction strategies or refinements intrinsically linked to updated wavefunction information. This implies a more classical approach: experiments validate and stimulate theoretical predictions and vice versa. In fact, crystallographic data contain information on a *real* system (which is in principle "unknown", defective, at a given temperature, etc.) and on a space/time averaged basis, whereas QM calculations refer to a *model* system (with a certain composition, geometry, Hamiltonian, etc.) and have both the advantages and the disadvantages of treating a well-defined, but approximate object.

In this view, QCr would be the branch of science studying the quantum mechanical functions (and properties derived from them) in crystals. This includes the investigation, in position or in momentum space, of charge and spin density, wavefunctions, density matrices, based on experiments, on theoretical calculations or on a combination of them.

III. Third option: Crystals as quantum objects

According to this view, QCr is the study of properties and phenomena that occur in crystalline matter and can be explained only by quantum mechanics. Again, a combination of experimental methodologies and theories describe, understand and predict those phenomena. In keeping with Feynman, the various theories concern especially the interaction between matter and radiation (which reveals the atomic and electronic structure of a compound) as well as the bonding between atoms or molecules (which dictates the electronic structure and explains the behavior of a material). The experimental methods include scattering and spectroscopic techniques, with observations enabling to refine quantum mechanical models that reveal structural or functional features. Specific goals of QCr are the determination of quantum related functions and quantities (such as wavefunctions, charge and spin densities, density matrices, electric or magnetic moments, etc.), the evaluation of the properties of materials and the analysis of the bonding features between the atoms and molecules that constitute a crystal.

This open definition reflects the broad definitions of quantum biology and quantum chemistry, i.e. the application of quantum mechanical concepts to chemical compounds and biologically relevant objects. This implies that QCr does not only include determination of wavefunctions, density matrices or electron densities, but, more generally, it concerns the study of electronic structures and their changes, including, for example, the determination of magnetic structures, photo-induced processes, electric and magnetic polarizations and polarizabilities, *etc.* In this definition, the simple determination of crystal structures is not *per se* a quantum crystallographic study, if the purpose is simply mechanical but not quantum-mechanical. In other words, the determination of a structure to provide a "ball and stick" picture of a molecule or a solid cannot be considered quantum crystallography, although quantum crystallographic methods may find application also for more general purposes (see also next section). On the other hand, determinations of structures of photo-excited species or (electric or magnetic) field-polarized compounds clearly belong to quantum crystallography. This open definition means that QCr is the field that bridges structure and functions through the distribution and dynamics of electrons in space.

IV. Fourth option: quantum crystallography as a multidisciplinary field.

If quantum crystallographic studies tackle all quantum mechanics-based problems in crystallography, then the possible connections with other disciplines are enormous. Molecular chemists, biochemists and solid-state chemists may take advantage of improved models for equilibrium structures at specific thermodynamic conditions. Material scientists may appreciate an improved knowledge of the dynamics of atomic and electronic structures under perturbation. Theoretical chemists will find new and more precise ways to test their theoretical models.

However, this concept of QCr is not limited to solid-state science, but also includes surface science as well as studies of nanoscale materials, e.g. via radiation-damage free femtosecond X-ray protein nanocrystallography[272-274] or via electron diffraction in thin films and monolayers.[275] Since QCr is inherently associated with scattering, an obvious extension of

the domain is the scattering and imaging of isolated (macro-)molecules or single objects such as cells,[276] which is nowadays feasible with new X-ray lasing or intense electron sources.[277-281] In this respect, we note that the term "quantum crystallography" has been also used for these kinds of studies.[56]

Risks and opportunities:

One of our goals is finding a new definition of QCr. However, this includes the inherent risk of confusing the new meaning/definition of QCr with the original one that has just recently been reviewed[44,45] or the risk of excluding new facets that will naturally emerge due to a continuous progress of crystallography and quantum mechanical methods. Therefore, it is important to dynamically fill the new definition with applications and examples in order to be acknowledged as useful and meaningful. This will allow beneficial interactions with neighboring research areas where important innovations are expected. This article intends to provide a first attempt to set the domain, to address the connections with other disciplines and the possible implications of quantum crystallographic studies. Strong synergies are expected with materials and life sciences, including many different fields of crystallography.

Acknowledgments:

The authors thank Hans-Beat Bürgi, Lukáš Palatinus, Wolfgang Scherer, Michael E. Wall, Bartolomeo Civalleri, Roberto Dovesi, Alessandro Erba and Silvia Casassa for their contributions to the discussion meeting in terms of their definitions and opinions about quantum crystallography.

Financial support for the discussion meeting by the Centre Européen de Calcul Atomique et Moléculaire, Bruker AXS GmbH, WIEN2k, TURBOMOLE GmbH, French Chemical Society (SCF), and Métropole du Grand Nancy is gratefully acknowledged.

A.G. acknowledges the French Research Agency (ANR) for financial support through the Grant No. ANR-17-CE29-0005.

L.B. acknowledges financial support from VEGA (grants Nos. 1/0598/16 and 1/0871/16) and APVV (grants Nos. APVV-15-0079 and APVV-15-0053).

E.E. acknowledges the French Research Agency (ANR) for financial support through the Grant ANR-08-BLAN-0091-01, CINES/CEA CCRT/IDRIS for allocation of computing time (project x2016087449) and his main collaborators Emmanuel Aubert, Ignasi Mata, Ibon Alkorta, Elies Molins and Marc Fourmigué.

C.G. gratefully acknowledges funding from Danmarks Grundforskningsfond (award No. DNRF93).

P.G. acknowledges support from the EU through the MaX Centre of Excellence (Grant No. 676598).

J.-M.G. gratefully acknowledges the collaboration of Saber Gueddida and Zeyin Yan.

P. M. acknowledges funding form the Swiss National Science Foundation (project 160157).

C.F.M acknowledges the *Natural Sciences and Engineering Research Council of Canada* (NSERC), *Canada Foundation for Innovation* (CFI), the *Lady Davis Fellowship Trusts & The Hebrew University of Jerusalem* and *Mount Saint Vincent University* for funding.

P.N.H.N. acknowledges the Australian Research Council for funding through the *Future Fellowships Scheme* (grant number FT110100427)

U.R. acknowledges financial support from the Swedish research council (project 2014-5540).

S.G. thanks *DFG* within Emmy Noether GR 4451/1-1.

Graphical Abstract Text and Picture

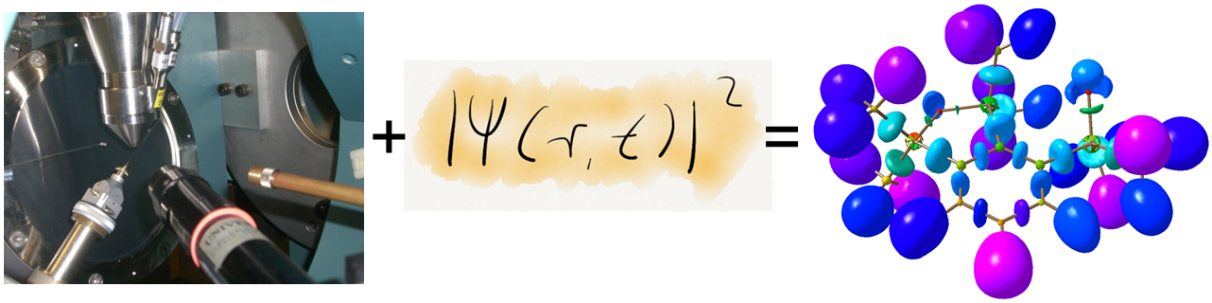

Between Two Worlds – A New World. An amalgamation of quantum mechanics and diffraction experiments is a magnifying lens for the quantum phenomena in molecules and materials. In this discussion paper, the new research domain "quantum crystallography" is debated in the context of current research fields. The perspective of becoming an independent natural science is outlined.

References

[1] A. H. Compton, *Nature* **1915**, *95*, 343–344.

[2] D. T. Cromer, *Acta Cryst.* **1965**, *19*, 224–227.

[3] G. M. Sheldrick, *Acta Cryst. A* **2008**, *64*, 112–122.

[4] J. C. Brooks-Bartlett, E. F. Garman, *Interdis. Sci. Rev.* **2015**, *40*, 244–264.

[5] P. Debye, *Ann. Phys.* **1915**, *351*, 809–823.

[6] P. Coppens, *Science* **1967**, *158*, 1577–1579.

[7] P. Coppens, *Angew. Chem. Int. Ed.* **2005**, *44*, 6810–6811.

[8] M. Sakata, M. Sato, *Acta Cryst. A* **1990**, *46*, 263–270.

[9] P. Roversi, J. J. Irwin, G. Bricogne, *Acta Cryst. A* **1998**, *54*, 971–996.

[10] S. van Smaalen, J. Netzel, *Phys. Scr.* **2009**, *79*, 048304.

[11] B. Dawson, *Proc. R. Soc. Lond. A* **1967**, *298*, 255–263.

[12] K. Kurki-Suonio, *Acta Cryst. A* **1968**, *24*, 379–390.

[13] F. L. Hirshfeld, *Acta Cryst. B* **1971**, *27*, 769–781.

[14] R. F. Stewart, *J. Chem. Phys.* **1969**, *51*, 4569–4577.

[15] N. K. Hansen, P. Coppens, *Acta Cryst. A* **1978**, *34*, 909–921.

[16] J. Bentley, R. F. Stewart, *J. Comput. Phys.* **1973**, *11*, 127–145.

[17] K. Tanaka, *Acta Cryst. A* **1988**, *44*, 1002–1008.

[18] J. R. Michael, T. Koritsanszky, *J. Math. Chem.* **2014**, *53*, 250–259.

[19] P. Coppens, *X-Ray Charge Densities and Chemical Bonding*, Oxford University Press, New York, **1997**.

[20] R. McWeeny, *Methods of Molecular Quantum Mechanics,*, Academic Press, London, **1992**.

[21] P. A. Holladay, P. Leung, P. Coppens, *Acta Cryst. A* **1983**, *39*, 377–387.

[22] J. Overgaard, *private communication*.

[23] M. Deutsch, B. Gillon, N. Claiser, J.-M. Gillet, C. Lecomte, M. Souhassou, *IUCrJ* **2014**, *1*, 194–199.

[24] L. Massa, L. Huang, J. Karle, *Int. J. Quantum Chem., Quantum Chem. Symp.* **1995**, *56*, 371–384.

[25] R. J. Weiss, *Physics Today* **2009**, *18*, 43–44.

[26] M. Cooper, *Phys. Scr.* **2015**, *91*, 012501.

[27] W. L. Clinton, L. J. Massa, *Phys. Rev. Lett.* **1972**, *29*, 1363–1366.

[28] D. Jayatilaka, *Phys. Rev. Lett.* **1998**, *80*, 798–801.

[29] D. Jayatilaka, D. J. Grimwood, *Acta Cryst. A* **2001**, *57*, 76–86.

[30] D. J. Grimwood, D. Jayatilaka, *Acta Cryst. A* **2001**, *57*, 87–100.

[31] D. J. Grimwood, I. Bytheway, D. Jayatilaka, *J. Comput. Chem.* **2003**, *24*, 470–483.

[32] D. Jayatilaka, in *Modern Charge-Density Analysis* (Eds.: C. Gatti, P. Macchi), Springer Netherlands, Dordrecht, **2012**, pp. 213–257.

[33] M. Hudák, D. Jayatilaka, L. Perašínová, S. Biskupič, J. Kožíšek, L. Bučinský, *Acta Cryst. A* **2010**, *66*, 78–92.

[34] L. Bučinský, D. Jayatilaka, S. Grabowsky, *J. Phys. Chem. A* **2016**, *120*, 6650–6669.

[35] A. Genoni, *J. Phys. Chem. Lett.* **2013**, *4*, 1093–1099.

[36] A. Genoni, *J. Chem. Theory Comput.* **2013**, *9*, 3004–3019.

[37] L. H. R. Dos Santos, A. Genoni, P. Macchi, *Acta Cryst. A* **2014**, *70*, 532–551.

[38] A. Genoni, B. Meyer, *Adv. Quantum Chem.* **2016**, *73*, 333–362.

[39] A. Genoni, *Acta Cryst. A* **2017**, *73*, 312–316.

[40] N. Casati, A. Genoni, B. Meyer, A. Krawczuk, P. Macchi, *Acta Cryst. B* **2017**, *73*, 584–597.

[41] J.-M. Gillet, P. J. Becker, *J. Phys. Chem. Sol.* **2004**, *65*, 2017–2023.

[42] J.-M. Gillet, *Acta Cryst. A* **2007**, *63*, 234–238.

[43] J.-M. Gillet, P. J. Becker, P. Cortona, *Phys. Rev. B* **2001**, *63*, 235115.

[44] V. Tsirelson, *J. Comput. Chem.* **2017**, *56*, DOI 10.1002/jcc.24893.

[45] S. Grabowsky, A. Genoni, H.-B. Bürgi, *Chem. Sci.* **2017**, *8*, 4159–4176.

[46] L. Huang, L. Massa, J. Karle, *Int. J. Quantum Chem.* **1999**, *73*, 439–450.

[47] D. J. H. Cockayne, P. Goodman, J. C. Mills, A. F. Moodie, *Rev. Sci. Instrum.* **1967**, *38*, 1097–1103.

[48] J. M. Cowley, *Acta Cryst. A* **1969**, *25*, 129–134.

[49] J. C. H. Spence, *Acta Cryst. A* **1993**, *49*, 231–260.

[50] M. Tanaka, *Acta Cryst. A* **1994**, *50*, 261–286.

[51] U. Ryde, L. Olsen, K. Nilsson, *J. Comput. Chem.* **2002**, *23*, 1058–1070.

[52] N. Yu, H. P. Yennawar, K. M. Merz Jr., *Acta Cryst. D* **2005**, *61*, 322–332.

[53] D. Jayatilaka, B. Dittrich, *Acta Cryst. A* **2008**, *64*, 383–393.

[54] S. C. Capelli, H.-B. Bürgi, B. Dittrich, S. Grabowsky, D. Jayatilaka, *IUCrJ* **2014**, *1*, 361–379.

[55] M. Zheng, J. R. Reimers, M. P. Waller, P. V. Afonine, *Acta Cryst. D* **2017**, *73*, 45–52.

[56] Z. Li, T. Peng, N. Medvedev, F. Wang, H. N. Chapman, Y. Shih, arXiv:1606.03517.

[57] L. Massa, C. F. Matta, *J. Comput. Chem.* **2017**, DOI 10.1002/jcc.25102.

[58] J. Yang, M. P. Waller, *J. Comput. Chem.* **2012**, *34*, 466–470.

[59] L. Piela, *Ideas of Quantum Chemistry*, Elsevier, Waltham, **2014**.

[60] P. Hohenberg, W. Kohn, *Phys. Rev.* **1964**, *136*, B864–B871.

[61] W. Kohn, L. J. Sham, *Phys. Rev.* **1965**, *140*, A1133–A1138.

[62] K. Schwarz, in *Selected Topics of Quantum Mechanics* (Ed.: M.R. Pahlavani), InTech, **2015**, pp. 275–310.

[63] D. M. Ceperley, B. J. Alder, *Phys. Rev. Lett.* **1980**, *45*, 566–569.

[64] J. P. Perdew, K. Burke, M. Ernzerhof, *Phys. Rev. Lett.* **1996**, *77*, 3865–3868.

[65] J. P. Perdew, A. Ruzsinszky, G. I. Csonka, O. A. Vydrov, G. E. Scuseria, L. A. Constantin, X. Zhou, K. Burke, *Phys. Rev. Lett.* **2008**, *100*, 136406.

[66] J. P. Perdew, S. Kurth, A. Zupan, P. Blaha, *Phys. Rev. Lett.* **1999**, *82*, 2544–2547.

[67] J. P. Perdew, M. Ernzerhof, K. Burke, *J. Chem. Phys.* **1996**, *105*, 9982–9985.

[68] F. Tran, P. Blaha, K. Schwarz, *J. Chem. Theory Comput.* **2015**, *11*, 4717–4726.

[69] P. Giannozzi, O. Andreussi, T. Brumme, O. Bunau, M. Buongiorno Nardelli, M. Calandra, R. Car, C. Cavazzoni, D. Ceresoli, M. Cococcioni, N. Colonna, I. Carnimeo, A. Dal Corso, S. De Gironcoli, P. Delugas, R. A. DiStasio Jr., A. Ferretti, A. Floris, G. Fratesi, G. Fugallo, R. Gebauer, U. Gerstmann, F. Giustino, T. Gorni, J. Jia, M. Kawamura, H.-Y. Ko, A. Kokalj, E. Küçükbenli, M. Lazzeri, M. Marsili, N. Marzari, F. Mauri, N. L. Nguyen, H.-V. Nguyen, A. Otero-de-la-Roza, L. Paulatto, S. Poncé, D. Rocca, R. Sabatini, B. Santra, M. Schlipf, A. P. Seitsonen, A. Smogunov, I. Timrov, T. Thonhauser, P. Umari, N. Vast, X. Wu, S. Baroni, *J. Phys.: Condens. Matter* **2017**, *29*, 465901.

[70] F. Furche, R. Ahlrichs, C. Hättig, W. Klopper, M. Sierka, F. Weigend, *WIREs Comp. Mol. Sci.* **2014**, *4*, 91–100.

[71] P. Blaha, K. Schwarz, G. Madsen, D. Kvasnicka, J. Luitz, *WIEN2k, An Augmented Plane Wave + Local Orbitals Program for Calculating Crystal Properties*, Technische Universität Wien, Vienna (Austria), **2001**.

[72] K. Lejaeghere, G. Bihlmayer, T. Björkman, P. Blaha, S. Blügel, V. Blum, D. Caliste, I. E. Castelli, S. J. Clark, A. Dal Corso, S. de Gironcoli, T. Deutsch, J. K. Dewhurst, I. Di Marco, C. Draxl, M. Dułak, O. Eriksson, J. A. Flores-Livas, K. F. Garrity, L. Genovese, P. Giannozzi, M. Giantomassi, S. Goedecker, X. Gonze, O. Grånäs, E. K. U. Gross, A. Gulans, F. Gygi, D. R. Hamann, P. J. Hasnip, N. A, W. Halzwarth, D. Iuşan, D. B. Jochym, F. Jollet, D. Jones, G. Kresse, K. Kopernik, E. Küçükbenli, Y. O. Kvashnin, I. L. M. Locht, S. Lubeck, M. Marsman, N. Marzari, U. Nitzsche, L. Nordström, T. Ozaki, L. Paulatto, C. J. Pickard, W. Poelmans, M. I. J. Probert, K. Refson, M. Richter, G. M. Rignanese, S. Saha, M. Scheffler, M. Schlipf, K. Schwarz, S. Sharma, F. Tavazza, P. Thunström, A. Tkatchenko, M. Torrent, D. Vanderbilt, M. J. van Setten, V. Van Speybroeck, J, M. Wills, J. R. Yates, G.-X. Zhang, S. Cottenier, *Science* **2016**, *351*, aad3000.

[73] C. Pisani, R. Dovesi, A. Erba, P. Giannozzi, in *Modern Charge-Density Analysis* (Eds.: C. Gatti, P. Macchi), Springer Netherlands, Dordrecht, **2012**, pp. 79–132.

[74] M. Sierka, in *Computational Modelling of Inorganic Nanomaterials* (Eds.: S.T. Bromley, M. Zwijnenburg), CRC Press, Boca Raton (Florida, U.S.A.), **2016**, pp. 335–367.

[75] E. Welchman, P. Giannozzi, T. Thonhauser, *Phys. Rev. B* **2014**, *89*, 180101.

[76] M. Woińska, D. Jayatilaka, B. Dittrich, R. Flaig, P. Luger, K. Woźniak, P. M. Dominiak, S. Grabowsky, *ChemPhysChem* **2017**, *56*, 371–3351.

[77] B. Hasse, J. N. Schmidt-May, F. Hertlein, P. Radcliffe, C. Michaelsen, *Proc. SPIE, Advances in Laboratory-based X-Ray Sources, Optics, and Applications VI* **2017**, *10387*, 103870B.

[78] M. R. V. Jørgensen, V. R. Hathwar, N. Bindzus, N. Wahlberg, Y.-S. Chen, J. Overgaard, B. B. Iversen, *IUCrJ* **2014**, *1*, 267–280.

[79] E. Frojdh, R. Ballabriga, M. Campbell, M. Fiederle, E. Hamann, T. Koenig, X. Llopart, D. de P. Magalhaes, M. Zuber, *J. Instrum.* **2014**, *9*, C04028.

[80] A. Schubert, G. J. O'Keefe, B. A. Sobott, N. M. Kirby, R. P. Rassool, *Radiat. Phys. Chem.* **2010**, *79*, 1111–1114.

[81] C. Ponchut, F. Zontone, H. Graafsma, *IEEE Trans. Nucl. Sci.* **2005**, *52*, 1760–1765.

[82] P. Denes, B. Schmitt, *J. Synchrotron Radiat.* **2014**, *21*, 1006–1010.

[83] L. Krause, R. Herbst-Irmer, G. M. Sheldrick, D. Stalke, *J. Appl. Cryst.* **2015**, *48*, 3–10.

[84] M. Mueller, M. Wang, C. Schulze-Briese, *Acta Cryst. D* **2012**, *68*, 42–56.

[85] G. Wu, B. L. Rodrigues, P. Coppens, *J. Appl. Cryst.* **2002**, *35*, 356–359.

[86] T. Schulz, K. Meindl, D. Leusser, D. Stern, J. Graf, C. Michaelsen, M. Ruf, G. M. Sheldrick, D. Stalke, *J. Appl. Cryst.* **2009**, *42*, 885–891.

[87] M. R. V. Jørgensen, H. Svendsen, M. S. Schmøkel, J. Overgaard, B. B. Iversen, *Acta Cryst. A* **2012**, *68*, 301–303.

[88] R. F. Stewart, *Acta Cryst. A* **1976**, *32*, 565–574.

[89] A. Fischer, D. Tiana, W. Scherer, K. Batke, G. Eickerling, H. Svendsen, N. Bindzus, B. B. Iversen, *J. Phys. Chem. A* **2011**, *115*, 13061–13071.

[90] T. S. Koritsanszky, P. Coppens, *Chem. Rev.* **2001**, *101*, 1583–1628.

[91] S. B. Novaković, G. A. Bogdanović, C. Heering, G. Makhloufi, D. Francuski, C. Janiak, *Inorg. Chem.* **2015**, *54*, 2660–2670.

[92] B. Dittrich, E. Sze, J. J. Holstein, C. B. Hübschle, D. Jayatilaka, *Acta Cryst. A* **2012**, *68*, 435–442.

[93] K. N. Jarzembska, K. Ślepokura, R. Kamiński, M. J. Gutmann, P. M. Dominiak, K. Woźniak, *Acta Cryst. B* **2017**, *73*, 550–564.

[94] N. Casati, A. Kleppe, A. P. Jephcoat, P. Macchi, *Nat. Commun.* **2016**, *7*, 10901.

[95] S. Pillet, V. Legrand, H.-P. Weber, M. Souhassou, J.-F. Létard, P. Guionneau, C. Lecomte, *Z. Kristallogr.* **2008**, *223*, 235–249.

[96] N. K. Hansen, P. Fertey, R. Guillot, *Acta Cryst. A* **2004**, *60*, 465–471.

[97] S. Gorfman, O. Schmidt, V. Tsirelson, M. Ziolkowski, U. Pietsch, *Z. Anorg. Allg. Chem.* **2013**, *639*, 1953–1962.

[98] S. Grabowsky, P. Luger, J. Buschmann, T. Schneider, T. Schirmeister, A. N. Sobolev, D. Jayatilaka, *Angew. Chem. Int. Ed.* **2012**, *51*, 6776–6779.

[99] H. Wolf, M. R. V. Jørgensen, Y.-S. Chen, R. Herbst-Irmer, D. Stalke, *Acta Cryst. B* **2015**, *71*, 10–19.

[100] A. M. Makal, D. Plażuk, J. Zakrzewski, B. Misterkiewicz, K. Woźniak, *Inorg. Chem.* **2010**, *49*, 4046–4059.

[101] P. García, S. Dahaoui, C. Katan, M. Souhassou, C. Lecomte, *Faraday Discuss.* **2007**, *135*, 217–235.

[102] S. Domagała, B. Fournier, D. Liebschner, B. Guillot, C. Jelsch, *Acta Cryst. A* **2012**, *68*, 337–351.

[103] B. Dittrich, C. B. Hübschle, K. Pröpper, F. Dietrich, T. Stolper, J. J. Holstein, *Acta Cryst. B* **2013**, *69*, 91–104.

[104] K. N. Jarzembska, P. M. Dominiak, *Acta Cryst. A* **2012**, *68*, 139–147.

[105] J. M. Bąk, S. Domagała, C. Hübschle, C. Jelsch, B. Dittrich, P. M. Dominiak, *Acta Cryst. A* **2011**, *67*, 141–153.

[106] J. R. Michael, T. Koritsanszky, *J. Chem. Phys.* **2017**, *146*, 204105.

[107] B. Dittrich, C. B. Hübschle, M. Messerschmidt, R. Kalinowski, D. Girnt, P. Luger, *Acta Cryst. A* **2005**, *61*, 314–320.

[108] M. Woińska, S. Grabowsky, P. M. Dominiak, K. Woźniak, D. Jayatilaka, *Sci. Adv.* **2016**, *2*, e1600192.

[109] B. Dittrich, J. Lübben, S. Mebs, A. Wagner, P. Luger, R. Flaig, *Chem. Eur. J.* **2017**, *23*, 4605–4614.

[110] M. Malischewski, K. Seppelt, J. Sutter, F. W. Heinemann, B. Dittrich, K. Meyer, *Angew. Chem. Int. Ed.* **2017**, *56*, 13372–13376.

[111] B. Fournier, E.-E. Bendeif, B. Guillot, A. Podjarny, C. Lecomte, C. Jelsch, *J. Am. Chem. Soc.* **2009**, *131*, 10929–10941.

[112] M. Malińska, K. N. Jarzembska, A. M. Goral, A. Kutner, K. Woźniak, P. M. Dominiak, *Acta Cryst. D* **2014**, *70*, 1257–1270.

[113] P. Kumar, S. A. Bojarowski, K. N. Jarzembska, S. Domagała, K. Vanommeslaeghe, A. D. MacKerell Jr., P. M. Dominiak, *J. Chem. Theory Comput.* **2014**, *10*, 1652–1664.

[114] S. A. Bojarowski, P. Kumar, P. M. Dominiak, *ChemPhysChem* **2016**, *17*, 2455–2460.

[115] V. A. Streltsov, P. N. H. Nakashima, A. W. S. Johnson, *J. Phys. Chem. Sol.* **2001**, *62*, 2109–2117.

[116] J. Friis, B. Jiang, J. Spence, K. Marthinsen, R. Holmestad, *Acta Cryst. A* **2004**, *60*, 402–408.

[117] A. B. Voufack, N. Claiser, C. Lecomte, S. Pillet, Y. Pontillon, B. Gillon, Z. Yan, J.-M. Gillet, M. Marazzi, A. Genoni, M. Souhassou, *Acta Cryst. B* **2017**, *73*, 544–549.

[118] W. L. Clinton, C. A. Frishberg, L. J. Massa, P. A. Oldfield, *Int. J. Quantum Chem., Quantum Chem. Symp.* **1973**, *7*, 505–514.

[119] C. Frishberg, L. J. Massa, *Phys. Rev. B* **1981**, *24*, 7018–7024.

[120] S. T. Howard, J. P. Huke, P. R. Mallinson, C. S. Frampton, *Phys. Rev. B* **1994**, *49*, 7124–7136.

[121] H. Schmider, V. H. Smith Jr., W. Weyrich, *J. Chem. Phys.* **1992**, *96*, 8986–8994.

[122] L. M. Pecora, *Phys. Rev. B* **1986**, *33*, 5987–5993.

[123] M. Cooper, P. Mijnarends, N. Shiotani, N. Sakai, A. Bansil, *X-Ray Compton Scattering*, Oxford University Press, Oxford, **2004**.

[124] M. Hillery, R. F. O'Connell, M. O. Scully, E. P. Wigner, in *The Collected Works of Eugene Paul Wigner, Volume IV, Part I: Physical Chemistry. Part II: Solid State Physics* (Ed.: A.S. Wightman), Berlin & Heidelberg, **1997**, pp. 273–317.

[125] S. Gueddida, J.-M. Gillet, *in preparation*.

[126] A. E. Whitten, D. Jayatilaka, M. A. Spackman, *J. Chem. Phys.* **2006**, *125*, 174505.

[127] D. Jayatilaka, P. Munshi, M. J. Turner, J. A. K. Howard, M. A. Spackman, *Phys. Chem. Chem. Phys.* **2009**, *11*, 7209–7218.

[128] D. D. Hickstein, J. M. Cole, M. J. Turner, D. Jayatilaka, *J. Chem. Phys.* **2013**, *139*, 064108.

[129] J. M. Cole, D. D. Hickstein, *Phys. Rev. B* **2013**, *88*, 302.

[130] A. Genoni, L. H. R. Dos Santos, B. Meyer, P. Macchi, *IUCrJ* **2017**, *4*, 136–146.

[131] K. C. Mondal, H. W. Roesky, A. C. Stückl, F. Ehret, W. Kaim, B. Dittrich, B. Maity, D. Koley, *Angew. Chem. Int. Ed.* **2013**, *52*, 11804–11807.

[132] F. L. Hirshfeld, *Isr. J. Chem.* **2013**, *16*, 198–201.

[133] F. L. Hirshfeld, *Theoret. Chim. Acta* **1977**, *44*, 129–138.

[134] M. Woińska, D. Jayatilaka, M. A. Spackman, A. J. Edwards, P. M. Dominiak, K. Woźniak, E. Nishibori, K. Sugimoto, S. Grabowsky, *Acta Cryst. A* **2014**, *70*, 483–498.

[135] B. Meyer, B. Guillot, M. F. Ruiz-Lopez, A. Genoni, *J. Chem. Theory Comput.*

2016, *12*, 1052–1067.

[136] B. Meyer, B. Guillot, M. F. Ruiz-Lopez, C. Jelsch, A. Genoni, *J. Chem. Theory Comput.* **2016**, *12*, 1068–1081.

[137] U. Ryde, *Dalton Trans.* **2007**, *50*, 607–625.

[138] K. M. Merz Jr., *Acc. Chem. Res.* **2014**, *47*, 2804–2811.

[139] G. J. Kleywegt, T. A. Jones, *Methods Enzymol.* **1997**, *277*, 208–230.

[140] U. Ryde, K. Nilsson, *J. Am. Chem. Soc.* **2003**, *125*, 14232–14233.

[141] K. Nilsson, U. Ryde, *J. Inorg. Biochem.* **2004**, *98*, 1539–1546.

[142] L. Rulíšek, U. Ryde, *J. Phys. Chem. B* **2006**, *110*, 11511–11518.

[143] P. Söderhjelm, U. Ryde, *J. Mol. Struct. (THEOCHEM)* **2006**, *770*, 199–219.

[144] O. Y. Borbulevych, J. A. Plumley, R. I. Martin, K. M. Merz Jr., L. M. Westerhoff, *Acta Cryst. D* **2014**, *70*, 1233–1247.

[145] K. Nilsson, H.-P. Hersleth, T. H. Rod, K. K. Andersson, U. Ryde, *Biophys. J* **2004**, *87*, 3437–3447.

[146] H.-P. Hersleth, Y.-W. Hsiao, U. Ryde, C. H. Görbitz, K. K. Andersson, *Biochem. J.* **2008**, *412*, 257–264.

[147] J. Heimdal, P. Rydberg, U. Ryde, *J. Phys. Chem. B* **2008**, *112*, 2501–2510.

[148] N. Källrot, K. Nilsson, T. Rasmussen, U. Ryde, *Int. J. Quantum Chem.* **2004**, *102*, 520–541.

[149] L. Cao, O. Caldararu, U. Ryde, *J. Phys. Chem. B* **2017**, *121*, 8242–8262.

[150] X. Li, S. A. Hayik, K. M. Merz Jr., *J. Inorg. Biochem.* **2010**, *104*, 512–522.

[151] Z. Fu, X. Li, Y. Miao, K. M. Merz Jr., *J. Chem. Theory Comput.* **2013**, *9*, 1686–1693.

[152] Z. Fu, X. Li, K. M. Merz Jr., *J. Chem. Theory Comput.* **2012**, *8*, 1436–1448.

[153] N. Yu, S. A. Hayik, B. Wang, N. Liao, C. H. Reynolds, K. M. Merz Jr., *J. Chem. Theory Comput.* **2006**, *2*, 1057–1069.

[154] X. Li, X. He, B. Wang, K. M. Merz Jr., *J. Am. Chem. Soc.* **2009**, *131*, 7742–7754.

[155] N. Yu, X. Li, G. Cui, S. A. Hayik, K. M. Merz Jr., *Protein Sci.* **2006**, *15*, 2773–

2784.

[156] F. Manzoni, O. Caldararu, E. Oksanen, D. T. Logan, U. Ryde, *J. Appl. Cryst.*, *in preparation*.

[157] Y.-W. Hsiao, T. R. Drakenberg, U. Ryde, *J. Biomol. NMR* **2005**, *31*, 97–114.

[158] B. Wang, L. M. Westerhoff, K. M. Merz Jr., *J. Med. Chem.* **2007**, *50*, 5128–5134.

[159] B. Wang, K. Raha, K. M. Merz Jr., *J. Am. Chem. Soc.* **2004**, *126*, 11430–11431.

[160] X. He, B. Wang, K. M. Merz Jr., *J. Phys. Chem. B* **2009**, *113*, 10380–10388.

[161] D. K. Chakravorty, B. Wang, C. W. Lee, A. J. Guerra, D. P. Giedroc, K. M. Merz Jr., *J. Biomol. NMR* **2013**, *56*, 125–137.

[162] B. Wang, K. M. Merz Jr., *J. Am. Chem. Soc.* **2005**, *127*, 5310–5311.

[163] D. E. Williams, M. B. Peters, B. Wang, A. E. Roitberg, K. M. Merz Jr., *J. Phys. Chem. A* **2009**, *113*, 11550–11559.

[164] Y.-W. Hsiao, Y. Tao, J. E. Shokes, R. A. Scott, U. Ryde, *Phys. Rev. B* **2006**, *74*, 358.

[165] U. Ryde, Y.-W. Hsiao, L. Rulíšek, E. I. Solomon, *J. Am. Chem. Soc.* **2007**, *129*, 726–727.

[166] X. Li, E. M. Sproviero, U. Ryde, V. S. Batista, G. Chen, *Int. J. Quantum Chem.* **2012**, *113*, 474–478.

[167] Y.-W. Hsiao, U. Ryde, *Inorg. Chim. Acta* **2006**, *359*, 1081–1092.

[168] X. Li, P. E. M. Siegbahn, U. Ryde, *Proc. Natl. Acad. Sci. U.S.A.* **2015**, *112*, 3979–3984.

[169] W. L. Clinton, A. J. Galli, L. J. Massa, *Phys. Rev.* **1969**, *177*, 7–13.

[170] L. Massa, *Chem. Script.* **1986**, *26*, 469–472.

[171] W. Polkosnik, L. Massa, *J. Comput. Chem.* **2017**, *31*, DOI 10.1002/jcc.25064.

[172] A. A. Hoser, A. Ø. Madsen, *Acta Cryst. A* **2016**, *72*, 206–214.

[173] A. A. Hoser, A. Ø. Madsen, *Acta Cryst. A* **2017**, *73*, 102–114.

[174] T. Aree, H.-B. Bürgi, *J. Phys. Chem. B* **2006**, *110*, 26129–26134.

[175] I. Sovago, A. A. Hoser, A. Ø. Madsen, *in preparation*.

[176] N. Wahlberg, A. Ø. Madsen, *J. Appl. Cryst.* **2017**, *50*, 1791–1799.

[177] N. F. Mott, H. S. W. Massey, *The Theory of Atomic Collisions*, Clarendon Press, Oxford, **1965**.

[178] J. M. Zuo, *Acta Cryst. A* **1993**, *49*, 429–435.

[179] M. Saunders, D. M. Bird, N. J. Zaluzec, W. G. Burgess, A. R. Preston, C. J. Humphreys, *Ultramicroscopy* **1995**, *60*, 311–323.

[180] K. Tsuda, M. Tanaka, *Acta Cryst. A* **1999**, *55*, 939–954.

[181] J. M. Zuo, M. Kim, M. O'Keeffe, J. C. H. Spence, *Nature* **1999**, *401*, 49–52.

[182] J. Friis, G. K. H. Madsen, F. K. Larsen, B. Jiang, K. Marthinsen, R. Holmestad, *J. Chem. Phys.* **2003**, *119*, 11359–11366.

[183] J. M. Zuo, *Rep. Prog. Phys.* **2004**, *67*, 2053–2103.

[184] X. H. Sang, A. Kulovits, J. M. K. Wiezorek, *Acta Cryst. A* **2010**, *66*, 694–702.

[185] P. N. H. Nakashima, B. C. Muddle, *Phys. Rev. B* **2010**, *81*, 115135.

[186] P. N. H. Nakashima, A. E. Smith, J. Etheridge, B. C. Muddle, *Science* **2011**, *331*, 1583–1586.

[187] P. N. H. Nakashima, A. W. S. Johnson, *Ultramicroscopy* **2003**, *94*, 135–148.

[188] P. N. H. Nakashima, *Struct. Chem.* **2017**, *28*, 1319–1332.

[189] J. M. Cowley, A. F. Moodie, *Acta Cryst.* **1957**, *10*, 609–619.

[190] F. Bloch, *Z. Physik* **1929**, *52*, 555–600.

[191] H. Bethe, *Ann. Phys.* **1928**, *392*, 55–129.

[192] K. Momma, F. Izumi, *J. Appl. Cryst.* **2011**, *44*, 1272–1276.

[193] R. F. W. Bader, *Atoms in Molecules: a Quantum Theory*, Clarendon Press, Oxford, U.K., **1990**.

[194] G. R. Runtz, R. F. W. Bader, R. R. Messer, *Can. J. Chem.* **1977**, *55*, 3040–3045.

[195] C. Gatti, *Z. Kristallogr.* **2005**, *220*, 399–457.

[196] X. Fradera, M. A. Austen, R. F. W. Bader, *J. Phys. Chem. A* **1999**, *103*, 304–314.

[197] C. F. Matta, *J. Comput. Chem.* **2014**, *35*, 1165–1198.

[198] I. Sumar, P. W. Ayers, C. F. Matta, *Chem. Phys. Lett.* **2014**, *612*, 190–197.

[199] R. F. W. Bader, C. Gatti, *Chem. Phys. Lett.* **1998**, *287*, 233–238.

[200] C. F. Matta, *Theor. Comput. Chem.* **2018**, *1124*, 1-14.

[201] E. R. Johnson, S. Keinan, P. Mori-Sánchez, J. Contreras-García, A. J. Cohen, W. Yang, *J. Am. Chem. Soc.* **2010**, *132*, 6498–6506.

[202] G. Saleh, C. Gatti, L. Lo Presti, J. Contreras-García, *Chem. Eur. J.* **2012**, *18*, 15523–15536.

[203] R. F. W. Bader, H. Essén, *J. Chem. Phys.* **1984**, *80*, 1943–1960.

[204] B. Silvi, A. Savin, *Nature* **1994**, *371*, 683–686.

[205] M. Kohout, *Int. J. Quantum Chem.* **2004**, *97*, 651–658.

[206] J. A. Sans, F. J. Manjon, A. L. Pereira, C. Popescu, A. Munoz, P. Rodriguez-Hernandez, J. Pellicer-Porres, V. P. Cuenca-Gotor, J. Contreras-García, V. Monteseguro-Padron, J. Ibanez, *in preparation*.

[207] H. Hellmann, *Einführung in Die Quantenchemie*, Franz Deuticke, Leipzig & Vienna, **1937**.

[208] R. P. Feynman, *Phys. Rev.* **1939**, *56*, 340–343.

[209] T. T. T. Bui, S. Dahaoui, C. Lecomte, G. R. Desiraju, E. Espinosa, *Angew. Chem. Int. Ed.* **2009**, *48*, 3838–3841.

[210] M. E. Brezgunova, E. Aubert, S. Dahaoui, P. Fertey, S. Lebègue, C. Jelsch, J. G. Ángyán, E. Espinosa, *Cryst. Growth Des.* **2012**, *12*, 5373–5386.

[211] M. E. Brezgunova, J. Lieffrig, E. Aubert, S. Dahaoui, P. Fertey, S. Lebègue, J. G. Ángyán, M. Fourmigué, E. Espinosa, *Cryst. Growth Des.* **2013**, *13*, 3283–3289.

[212] K. Lamberts, P. Handels, U. Englert, E. Aubert, E. Espinosa, *CrystEngComm* **2016**, *18*, 3832–3841.

[213] E. Aubert, E. Espinosa, I. Nicolas, O. Jeannin, M. Fourmigué, *Faraday Discuss.* **2017**, *203*, 389–406.

[214] I. Mata, E. Molins, E. Espinosa, *J. Phys. Chem. A* **2007**, *111*, 9859–9870.

[215] I. Mata, I. Alkorta, E. Molins, E. Espinosa, *ChemPhysChem* **2012**, *13*, 1421–1424.

[216] I. Mata, I. Alkorta, E. Molins, E. Espinosa, *Chem. Phys. Lett.* **2013**, *555*, 106–109.

[217] I. Mata, E. Molins, I. Alkorta, E. Espinosa, *J. Phys. Chem. A* **2015**, *119*, 183–194.

[218] I. Alkorta, I. Mata, E. Molins, E. Espinosa, *Chem. Eur. J.* **2016**, *22*, 9226–9234.

[219] I. Mata, E. Molins, I. Alkorta, E. Espinosa, *J. Phys. Chem. A* **2007**, *111*, 6425–6433.

[220] M. Deutsch, N. Claiser, S. Pillet, Y. Chumakov, P. Becker, J.-M. Gillet, B. Gillon, C. Lecomte, M. Souhassou, *Acta Cryst. A* **2012**, *68*, 675–686.

[221] I. A. Kibalin, Z. Yan, A. B. Voufack, S. Gueddida, B. Gillon, A. Gukasov, F. Porcher, A. M. Bataille, F. Morini, N. Claiser, M. Souhassou, C. Lecomte, J.-M. Gillet, M. Ito, K. Suzuki, H. Sakurai, Y. Sakurai, C. M. Hoffmann, X. P. Wang, *Phys. Rev. B* **2017**, *96*, 054426.

[222] C. Gatti, G. Macetti, L. Lo Presti, *Acta Cryst. B* **2017**, *73*, 565–583.

[223] Z. Yan, I. A. Kibalin, N. Claiser, S. Gueddida, B. Gillon, A. Gukasov, A. B. Voufack, F. Morini, Y. Sakurai, M. Brancewicz, M. Itou, M. Itoh, N. Tsuji, M. Ito, M. Souhassou, C. Lecomte, P. Cortona, J-M. Gillet, *Phys. Rev. B* **2017**, *96*, 054427.

[224] C. Gatti, P. Macchi, in *Modern Charge-Density Analysis* (Eds.: C. Gatti, P. Macchi), Springer Netherlands, Dordrecht, **2012**, pp. 1–78.

[225] U. Flierler, D. Stalke, L. J. Farrugia, in *Modern Charge-Density Analysis* (Eds.: C. Gatti, P. Macchi), Springer Netherlands, Dordrecht, **2012**, pp. 435–467.

[226] A. M. Pendás, E. Francisco, M. A. Blanco, C. Gatti, *Chem. Eur. J.* **2007**, *13*, 9362–9371.

[227] P. Golub, A. I. Baranov, *J. Chem. Phys.* **2016**, *145*, 154107.

[228] A. I. Baranov, M. Kohout, *J. Comput. Chem.* **2011**, *32*, 2064–2076.

[229] A. D. Becke, K. E. Edgecombe, *J. Chem. Phys.* **1990**, *92*, 5397–5403.

[230] A. M. Pendás, M. Kohout, M. A. Blanco, E. Francisco, in *Modern Charge-Density Analysis* (Eds.: C. Gatti, P. Macchi), Springer Netherlands, Dordrecht, **2012**, pp. 303–358.

[231] R. Ponec, *J. Math. Chem.* **1997**, *21*, 323–333.

[232] R. Ponec, *J. Math. Chem.* **1998**, *23*, 85–103.

[233] C. Gatti, in *Electron Density and Chemical Bonding II. Structure and Bonding* (Ed.: D. Stalke), **2012**, pp. 193–285.

[234] M. Sironi, A. Genoni, M. Civera, S. Pieraccini, M. Ghitti, *Theor. Chem. Acc.* **2007**, *117*, 685–698.

[235] E. D. Glendening, C. R. Landis, F. Weinhold, *WIREs Comp. Mol. Sci.* **2011**, *2*, 1–42.

[236] N. Marzari, A. A. Mostofi, J. R. Yates, I. Souza, D. Vanderbilt, *Rev. Mod. Phys.* **2012**, *84*, 1419–1475.

[237] K. Finzel, *Int. J. Quantum Chem.* **2014**, *114*, 1546–1558.

[238] W. Scherer, G. Eickerling, C. Hauf, M. Presnitz, E.-W. Scheidt, V. Eyert, R. Pöttgen, in *Modern Charge-Density Analysis* (Eds.: C. Gatti, P. Macchi), Springer Netherlands, Dordrecht, **2012**, pp. 359–385.

[239] J. Zhang, L. Song, G. K. H. Madsen, K. F. F. Fischer, W. Zhang, X. Shi, B. B. Iversen, *Nat. Commun.* **2016**, *7*, 10892.

[240] B. Niepötter, R. Herbst-Irmer, D. Kratzert, P. P. Samuel, K. C. Mondal, H. W. Roesky, P. Jerabek, G. Frenking, D. Stalke, *Angew. Chem. Int. Ed.* **2014**, *53*, 2766–2770.

[241] L.-C. Wu, C.-W. Hsu, Y.-C. Chuang, G.-H. Lee, Y.-C. Tsai, Y. Wang, *J. Phys. Chem. A* **2011**, *115*, 12602–12615.

[242] E. Ressouche, *Phys. B Condens. Matter* **1999**, *267-268*, 27–36.

[243] J. X. Boucherle, B. Gillon, J. Maruani, J. Schweizer, *Mol. Phys.* **1987**, *60*, 1121–1142.

[244] E. Ressouche, J. X. Boucherle, B. Gillon, P. Rey, J. Schweizer, *J. Am. Chem. Soc.* **1993**, *115*, 3610–3617.

[245] L. H. R. Dos Santos, A. Lanza, A. M. Barton, J. Brambleby, W. J. A. Blackmore, P. A. Goddard, F. Xiao, R. C. Williams, T. Lancaster, F. L. Pratt, S. J. Blundell, J. Singleton, J. L. Manson, P. Macchi, *J. Am. Chem. Soc.* **2016**, *138*, 2280–2291.

[246] W. Volksen, R. D. Miller, G. Dubois, *Chem. Rev.* **2010**, *110*, 56–110.

[247] J.-G. Liu, M. Ueda, *J. Mater. Chem.* **2009**, *19*, 8907–8919.

[248] L. H. R. Dos Santos, A. Krawczuk, P. Macchi, *J. Phys. Chem. A* **2015**, *119*, 3285–3298.

[249] T. Elsaesser, M. Woerner, in *Modern Charge-Density Analysis* (Eds.: C. Gatti, P. Macchi), Springer Netherlands, Dordrecht, **2012**, pp. 697–714.

[250] J. Overgaard, Y. Grin, M. Takata, B. B. Iversen, in *Modern Charge-Density Analysis* (Eds.: C. Gatti, P. Macchi), Springer Netherlands, Dordrecht, **2012**, pp. 469–504.

[251] J. Maddox, *Nature* **1988**, *335*, 201.

[252] A. Gavezzotti, *Acc. Chem. Res.* **1994**, *27*, 309–314.

[253] A. R. Oganov, *Modern Methods of Crystal Structure Prediction*, Wiley-VCH Verlag GmbH & Co. KGaA, Weinheim, Germany, **2010**.

[254] A. R. Oganov, J. Chen, C. Gatti, Y. Ma, Y. Ma, C. W. Glass, Z. Liu, T. Yu, O. O. Kurakevych, V. L. Solozhenko, *Nature* **2009**, *457*, 863–867.

[255] Y. Ma, M. Eremets, A. R. Oganov, Y. Xie, I. Trojan, S. Medvedev, A. O. Lyakhov, M. Valle, V. Prakapenka, *Nature* **2009**, *458*, 182–185.

[256] X. Dong, A. R. Oganov, A. F. Goncharov, E. Stavrou, S. Lobanov, G. Saleh, G.-R. Qian, Q. Zhu, C. Gatti, V. L. Deringer, R. Dronskowski, X.-F. Zhou, V. Prakapenka, Z. Konôpková, I. Popov, A. I. Boldyrev & H.-T. Wang, *Nat. Chem.* **2017**, *9*, 440–445.

[257] W. Zhang, A. R. Oganov, A. F. Goncharov, Q. Zhu, S. E. Boulfelfel, A. O. Lyakhov, E. Stavrou, M. Somayazulu, V. B. Prakapenka, Z. Konopkova, *Science* **2013**, *342*, 1502–1505.

[258] Q. Zhu, A. R. Oganov, X.-F. Zhou, in *Prediction and Calculation of Crystal Structures* (Eds.: S. Atahan-Evrenk, A. Aspuru-Guzik), Springer International Publishing, Cham, **2014**, pp. 223–256.

[259] P. Mori-Sánchez, A. J. Cohen, W. Yang, *Phys. Rev. Lett.* **2008**, *100*, 146401.

[260] E. S. Kryachko, in *Applications of Density Functional Theory to Biological and Bioinorganic Chemistry. Structure and Bonding* (Eds.: M.V. Putz, M.D.P. Mingos), **2013**, pp. 65–96.

[261] J. P. Perdew, A. Ruzsinszky, *Rev. Mineral. Geochem.* **2010**, *71*, 1–18.

[262] J. S. Tse, E. V. Boldyreva, in *Modern Charge-Density Analysis* (Eds.: C. Gatti, P. Macchi), Springer Netherlands, Dordrecht, **2012**, pp. 573–623.

[263] J. Contreras-García, M. Marqués, B. Silvi, J. M. Recio, in *Modern Charge-Density Analysis* (Eds.: C. Gatti, P. Macchi), Springer Netherlands, Dordrecht, **2012**, pp. 625–658.

[264] P. L. A. Popelier, in *Applications of Topological Methods in Molecular Chemistry* (Eds.: R. Chauvin, C. Lepetit, B. Silvi, E. Alikhani), Cham (Switzerland), **2016**, pp. 23–52.

[265] M. Jacoby, *Chem. Eng. News* **2017**, *95*, 5–6.

[266] R. P. Feynman, R. B. Leighton, M. Sands, *The Feynman Lecture on Physics, Vol. III*, Addison-Wesley, Reading (Massachusetts, U.S.A.), **1964**.

[267] A. Erba, J. Baima, I. Bush, R. Orlando, R. Dovesi, *J. Chem. Theory Comput.* **2017**, *13*, 5019–5027.

[268] G. Kresse, J. Hafner, *Phys. Rev. B* **1993**, *47*, 558–561.

[269] G. Kresse, J. Hafner, *Phys. Rev. B* **1994**, *49*, 14251–14269.

[270] G. Kresse, J. Furthmüller, *Comput. Mater. Sci.* **1996**, *6*, 15–50.

[271] G. Kresse, J. Furthmüller, *Phys. Rev. B* **1996**, *54*, 11169–11186.

[272] H. N. Chapman, P. Fromme, A. Barty, T. A. White, R. A. Kirian, A. Aquila, M. S. Hunter, J. Schulz, D. P. DePonte, U. Weierstall, R. B. Doak, F. R. Maia, A. V. Martin, I. Schlichting, L. Lomb, N. Coppola, R. L. Shoeman, S. W. Epp, R. Hartmann, D. Rolles, A. Rudenko, L. Foucar, N. Kimmel, G. Weidenspointner, P. Holl, M. Liang, M. Barthelmess, C. Caleman, S. Boutet, M. J. Bogan, J. Krzywinski, C. Bostedt, S. Bajt, L. Gumprecht, B. Rudek, B. Erk, C. Schmidt, A. Hömke, C. Reich, D. Pietschner, L. Strüder, G. Hauser, H. Gorke, J. Ullrich, S.

Herrmann, G. Schaller, F. Schopper, H. Soltau, K. U. Kühnel, M. Messerschmidt, J. D. Bozek, S. P. Hau-Riege, M. Frank, C. Y. Hampton, R. G. Sierra, D. Starodub, G. J. Williams, J. Hajdu, N. Timneanu, M. M. Seibert, J. Andreasson, A. Rocker, O. Jönsson, M. Svenda, S. Stern, K. Nass, R. Andritschke, C. D. Schröter, F. Krasniqi, M. Bott, K. E. Schmidt, X. Wang, I. Grotjohann, J. M. Holton, T. R. Barends, R. Neutze, S. Marchesini, R. Fromme, S. Schorb, D. Rupp, M. Adolph, T. Gorkhover, I. Andersson, H. Hirsemann, G. Potdevin, H. Graafsma, B. Nilsson, J. C. H. Spence, *Nature* **2011**, *470*, 73–77.

[273] P. Fromme, J. C. Spence, *Curr. Opin. Struct. Biol.* **2011**, *21*, 509–516.

[274] K. Hirata, K. Shinzawa-Itoh, N. Yano, S. Takemura, K. Kato, M. Hatanaka, K. Muramoto, T. Kawahara, T. Tsukihara, E. Yamashita, K. Tono, G. Ueno, T. Hikima, H. Murakami, Y. Inubushi, M. Yabashi, T. Ishikawa, M. Yamamoto, T. Ogura, H. Sugimoto, J.-R. Shen, S. Yoshikawa, H. Ago, *Nat. Methods* **2014**, *11*, 734–736.

[275] D. S. Badali, R. Y. N. Gengler, R. J. D. Miller, *Struct. Dyn.* **2016**, *3*, 034302.

[276] P. Thibault, V. Elser, C. Jacobsen, D. Shapiro, D. Sayre, *Acta Cryst. A* **2006**, *62*, 248–261.

[277] K. Ayyer, O. M. Yefanov, D. Oberthür, S. Roy-Chowdhury, L. Galli, V. Mariani, S. Basu, J. Coe, C. E. Conrad, R. Fromme, A. Schaffer, K. Dörner, D. James, C. Kupitz, M. Metz, G. Nelson, P. L. Xavier, K. R. Beyerlein, M. Schmidt, I. Sarrou, J. C. H. Spence, U. Weierstall, T. A. White, J.-H. Yang, Y. Zhao, M. Liang, A. Aquila, M. S. Hunter, J. S. Robinson, J. E. Koglin, S. Boutet, P. Fromme, A. Barty, H. N. Chapman, *Nature* **2016**, *530*, 202–206.

[278] K. Ayyer, G. Geloni, V. Kocharyan, E. Saldin, S. Serkez, O. Yefanov, I. Zagorodnov, *Struct. Dyn.* **2015**, *2*, 041702.

[279] A. Fratalocchi, G. Ruocco, *Phys. Rev. Lett.* **2011**, *106*, 105504.

[280] R. J. D. Miller, R. Ernstorfer, M. Harb, M. Gao, C. T. Hebeisen, H. Jean-Ruel, C. Lu, G. Moriena, G. Sciaini, *Acta Cryst. A* **2010**, *66*, 137–156.

[281] M. Gao, C. Lu, H. Jean-Ruel, L. C. Liu, A. Marx, K. Onda, S.-Y. Koshihara, Y. Nakano, X. Shao, T. Hiramatsu, G. Saito, H. Yamochi, R. R. Cooney, G. Moriena, G. Sciaini, R. J. D. Miller, *Nature* **2013**, *496*, 343–346.